POLITECNICO DI TORINO

Master Degree in Biomedical Engineering

The Impact of Amyloid Beta Assembly on Membrane Conformational Stability and Dynamics

Thesis Supervisor   **Candidate**

Prof. M. A. Deriu   Chiara Lionello

Co-Supervisors

Prof. U. Morbiducci

Prof. J. A. Tuszynski

ACADEMIC YEAR 2018-2019

Contents

ABSTRACT

Alzheimer's disease (AD) is a neurodegenerative disorder that cause irreversible loss of neurons. Currently there are no treatments able to slow down or cure this disease. In fact, despite it is the most common form of dementia, the mechanism by which AD develops is still unclear. One of the hypotheses is based on the aggregation and the accumulation of amyloid β (Aβ) peptide around neuronal cells. Aβ peptide is present in two different forms: $A\beta_{40}$ and $A\beta_{42}$. The first one is the most abundant in amyloid plaques and can assume only a U-shaped structure, the second one is the most toxic and can assume also S-shaped structure, which is more stable and compact. Changes in Aβ metabolism lead to amyloid plaque formation which involves inflammatory response, neuronal injury and hyperphosphorylation of tau protein. Neuronal disfunction and cell death give rise to dementia onset.

Amyloid aggregates interact with the cell membrane producing toxic effects on the normal cell functions and activities. In particular, amyloid peptides are able to disrupt the cell membrane carpeting on its surface, generating transmembrane pores or disrupting the bilayer with a detergent-like behaviour. Small assemblies, especially small oligomers, seem to destabilize more the membrane. Analysis on membrane mechanics is useful to better understand the effects of the interactions between amyloid aggregates and lipid bilayer.

Molecular Dynamics simulations allow to focus on molecular phenomena related to neurodegenerative diseases. The present work has the purpose to study the effect of both ordered and disordered $A\beta_{11\text{-}42}$ pentamer inserted into POPC bilayer. Principal differences found concern the membrane order parameter and the bending modulus. Both properties decrease inversely proportional to the distance from the protein.

ESTRATTO

Il morbo di Alzheimer (AD) è una malattia neurodegenerativa che causa una perdita irreversibile di neuroni. Attualmente non esistono trattamenti in grado di rallentare o curare questa patologia, infatti, nonostante l'Alzheimer sia la forma di demenza più comune, non è ancora chiaro il meccanismo di insorgenza. Una delle ipotesi principali si basa sull'aggregazione e l'accumulazione di peptidi β amiloidi (Aβ) intono alle cellule neuronali. Esistono due forme diverse di peptide Aβ: $A\beta_{40}$ e $A\beta_{42}$. La prima è la più abbondante nelle placche amiloidi e può assumere esclusivamente una struttura a U, la seconda è più tossica e può assumere anche una forma a S, che è più stabile e compatta. Cambiamenti nel metabolismo della proteina Aβ comportano la formazione di placche che causano una risposta infiammatoria, il danneggiamento dei neuroni e l'iperfosforilazione delle proteine tau. La disfunzione neuronale e la morte delle cellule causano l'insorgenza della demenza.

Aggregati di peptidi amiloidi interagiscono con la membrana cellulare producendo effetti tossici sulle normali funzioni e attività cellulari. In particolare, i peptidi amiloidi sono in grado di distruggere la membrana cellulare causando muovendosi sulla sua superficie, generando canali ionici transmembrana e distruggendo il doppio strato fosfolipidico comportandosi come un detergente. Piccoli aggregati, specialmente piccoli oligomeri, sembrano destabilizzare maggiormente la membrana cellulare. Analizzare le proprietà meccaniche della membrana è utile per capire meglio gli effetti dell'iterazione tra la proteina e i lipidi.

Le simulazioni di dinamica molecolare permettono di focalizzare l'attenzione su questo meccanismo alla microscala. Questo lavoro ha l'obiettivo di studiare l'effetto di pentameri $A\beta_{11-42}$, sia ordinati che disordinati, inseriti all'interno di un doppio strato di lipidi POPC. Le differenze principali riscontrate riguardano il parametro d'ordine della membrana e il suo modulo di bending. Infatti, entrambe le proprietà mostrano un andamento inversamente proporzionale alla distanza dalla proteina.

Chapter 1

INTRODUCTION

This chapter introduces the present Master Thesis work and elucidates aims and objectives.

Alzheimer's disease (AD) is a neurodegenerative disorder that in 2015 caused 110,561 deaths in USA, becoming the sixth leading cause of death in the Unites States and the fifth leading cause of death in Americans older than 65 years[1]. Actually, there is not a cure and the only drugs available are able to treat and to slow AD symptoms preserving neurotransmitters.

Despite AD is the most common form of dementia, the mechanism of its onset is not yet completely understood. Different hypotheses of AD development have been proposed: the cholinergic hypothesis, the tau hypothesis, the amyloid cascade hypothesis and, recently, the vascular hypothesis. The most accredited hypothesis is based on the amyloid cascade, which considers the abnormal aggregation of amyloid β (Aβ) peptide and its accumulation in and around neuronal cells as the main cause of the dementia onset. Aβ peptide can assume two principal forms: $A\beta_{40}$ and $A\beta_{42}$. The former, constituted by 40 residues, is the most present in amyloid plaques and can assume only a U-shaped structure. The latter, composed by 42 residues, is less abundant but aggregates more rapidly and can assume also a S-shaped configuration, that is more compact and toxic. Alterations on Aβ metabolism are responsible of Aβ oligomerization and amyloid plaques formations and lead to an inflammatory response and synaptic injuries. This cascade of events and the hyperphosphorylation of tau protein cause neuronal disfunction and cell death associated with memory loss.

Amyloid peptides tend to aggregate originating ordered fibres and disordered oligomers. Small amyloid assembly can interact with neuronal membrane modifying normal cell activity and influencing protein misfolding and aggregation. Amyloid aggregates interact with the cellular membrane in three different ways: carpeting on the surface, generating transmembrane oligomeric pores and causing the detergent-like dissolution. The bilayer damage is a consequence of their combination, as each mechanism is associated to a different step of protein aggregation. The carpet and the detergent-like models occur when the protein is in form of monomer or small oligomer, while the assemblies' interaction with specific membrane receptor causes the pore formation. The bilayer composition affects the ability of the protein to adhere to the membrane. Since electrostatic interactions are the principal

driving forces in this process, there is a different affinity depending on the types of lipids constituting the lipid bilayer. In particular, a tendency of the protein to interact with non-pure phospholipid bilayer is observed. Furthermore, there are conflicting opinions regarding the presence of cholesterol. If on one side cholesterol increases the rigidity of the membrane hindering the insertion of the aggregate, on the other hand it increases the variance of the bilayer composition favouring the interaction by the protein.

Since current experimental techniques do not allow to study this interaction at atomic resolution, Molecular Dynamics (MD) simulations can be used to analyse this phenomenon at the microscopic scale. This work focuses on the consequences of interaction between amyloid aggregates and lipid membrane. In particular, a peptide, an oligomer and a fibre are inserted into POPC bilayer. Both effects of bilayer on protein misfolding and of aggregates on membrane conformational stability and dynamics are studied.

The chapters that compose this work are summarized below:

Chapter 1 is the present introductory part.

Chapter 2 shows in a general way Material and Methods used in this work. Sections 2.1 introduces the concept of molecular modelling applied on biological mechanism, Section 2.2 explains how Molecular Mechanics allows to implement molecular modelling, Section 2.3 presents the basics of Molecular Dynamics, in particular statistical ensemble and the implementation scheme, and, in conclusion, Section 2.4 includes methods actually used to analyse the membrane mechanics.

Chapter 3 contains an introduction to the pathology, its related consequences and the principal hypothesis developed to try to explain the mechanism of AD onset. Subsequently, the amyloid peptide and its ability to aggregate in more or less ordered assemblies are studied. The different methods with which amyloid proteins interact with the membrane and how these interactions vary according to the type of lipid that constitutes the bilayer and the presence of different concentrations of cholesterol are then investigated.

Chapter 4 contains the impact of Aβ assembly on membrane conformational stability and dynamics. Proteins do not undergo significant changes when they are inserted in membrane respect to when simulated in solution. Regarding the membrane, oligomer and fibre tend to modify more its properties. In particular, aggregates influence in the same way the area per lipid and the bilayer thickness, while different consequences are observed for tilt and splay

angle. Variations on order parameter and bending modulus depend on the distance from the proteins' centre of mass.

Chapter 5 describes possible future developments of this work.

Chapter 2

MATERIALS AND METHODS

In this chapter a complete overview about computational methods for molecular modelling is presented explaining the physical basis behind the computational approach. Molecular dynamics simulations are used to study the impact of amyloid assemblies on membrane conformational stability and dynamics. Particular attention is given to mechanical properties, investigating the innovative methods that exploits all atoms Molecular Dynamics simulation.

2.1   Computational modelling of biomolecular systems

Models are used by scientists to study, with a certain degree of confidence, different phenomenon of the real word solving mathematical equations. Modelling permits to describe different aspects of reality, their interaction and dynamics. Acting on the model approximation, different levels of investigation are reached.

Molecular modelling consists of theoretical methods and computational techniques able to describe the behaviour of complex chemical systems (e.g., membranes, proteins, molecules) solving the equations of quantum and classical physics. At the quantum level, Schrodinger equation is solved to obtain a most detailed analysis. However, the Schrodinger equation can be solved only for simple systems, but molecular systems are characterized by an enormous number of molecules that is too large to be considered by quantum mechanics[2]. In fact, quantum mechanical methods consider relationships between the electrons in the system. This problem can be solved using Molecular Mechanics (MM), based on the Force Field methods (FF). This method ignores the electronic motions and calculate the energy of a system as a function of the coordinate of the nuclear position and can be used on systems containing significant number of atoms. Molecular Dynamics (MD) exploits FF to produce a dynamical trajectory of the system by the iterative integration of Newton's equations of motion.

MM and MD are explained exhaustively in the next sections.

2.2   Molecular mechanics

In Molecular Mechanics (MM), differently to Quantum Mechanics, atoms are treated as spheres whose mass depends on the elements and bonds are considered as springs whose stiffness depends on the elements bonded together. MM solves Newton's equations to study

an interacting molecular system. A set of equations, named forcefield (FF), permits to estimate the potential energy of the system only using the atoms' position.

2.2.1 Potential energy function

The potential energy function, obtained from the FF, can be considered as a sum of two individual energy contribution, in function of position:

$$V = V_{bonded} + V_{non-bonded}$$

The covalent and non-covalent terms are obtained from the following equations:

$$V_{bonded} = V_{bonds} + V_{angles} + V_{dihedrals}$$

$$V_{non-bonded} = V_{electrostatic} + V_{Van\ der\ Waals}$$

2.2.2 Treatment of Bond and Non-Bond interactions

In MM atoms are described as spheres and bonds are represented as springs. The potential energy function (Figure 1) can be described in terms of atom position (r) and number of atoms (N):

$$V(r^N) = \sum_{bonds} \frac{k_l}{2}(l - l_0)^2 + \sum_{angles} \frac{k_\theta}{2}(\theta - \theta_0)^2 + \sum_{torsions} k_\phi(1 + \cos(n\phi - \delta))$$

$$+ \sum_{i=1}^{N} \sum_{j=i+1}^{N} \left(4\varepsilon_{ij} \left[\left(\frac{\sigma_{ij}}{r_{ij}} \right)^{12} - \left(\frac{\sigma_{ij}}{r_{ij}} \right)^{6} \right] + \frac{q_i q_j}{4\pi\varepsilon_0 r_{ij}} \right)$$

The first term is referred to covalent bond that develops between two atoms. Bonds are modelled as a harmonic interaction, where k_l is the force constant, l_0 the reference bond length and l the bond length. The second term indicates the interactions between three atoms. Angles are described with a harmonic interaction, where k_θ is the force constant, θ_i the reference bond angle and θ the bond angle.

The third term is for dihedral angles which originates between four atoms. Torsions are described as a series of cosines, where k_ϕ is the energy barrier related to the angle deformation, n the multiplicity and δ the minimum position for torsional angle. This term includes both proper and improper dihedrals.

The last term is referred to the non-bonded interaction, that develops when molecules are near enough to influence each other. This term is divided in two parts, the first one describes Van der Waals forces, the second one electrostatic interaction.

Van der Waals potential is the weakest intermolecular force that originated between non-charged atoms. In act both at long and short range; at long range works as a temporary attractive force, at short range prevents the overlap between atom. Van der Waals forces are described with Lennard-Jones equation [3]:

$$V(r) = 4\varepsilon_{ij} \left[\left(\frac{\sigma_{ij}}{r_{ij}} \right)^{12} - \left(\frac{\sigma_{ij}}{r_{ij}} \right)^{6} \right]$$

Electrostatics interaction developed between charged atoms and are considered as long-range interactions. This force is described by Coulomb law:

$$V(r) = \frac{q_i q_j}{4\pi\varepsilon_0 r_{i,j}}$$

The number of non-bonded interactions increase as the square of the number of atoms in the system, this leads to an expensive computational effort. To solve this problem the non-bonded interactions are computed applying a *cutoff distance*. The non-bonded interactions are computed only if the atoms distance is smaller than the cutoff.


Figure 1 – Schematic representation of each term constituent the equation of the potential energy function.

2.2.3 Periodic Boundary Conditions

In MM the system is composed by the molecular model placed in a box filled by implicit or explicit models of water. Box boundaries represent a crucial issue in simulations because of the influence on properties of the whole system. Periodic Boundaries Conditions (PBC) allow to avoid side effects in case of both smaller and bigger boxes. Box is surrounded by copies of itself (Figure 2). Each particle in the box interacts with the other particles in adjacent boxes. Applying a Lennard-Jones cutoff is an artificial but avoid the interactions between a particle and itself in adjacent box. In fact, with PBC cutoff distance should be small enough to avoid a particle seeing itself in the adjacent box, this is named Minimum Image Convention. However, the presence of PBC may results in errors but are less severe than errors from unnatural interactions.

It is not a problem to apply a cutoff distance for short-range interaction. In case of long-range interaction, it can lead to discontinuities in the potential energy calculation. To solve this problem is necessary to use most accurate methods to properly evaluate the electrostatics interaction: Particle Mesh Ewalds[4], Reaction Field[5], Multipole Cells[6].
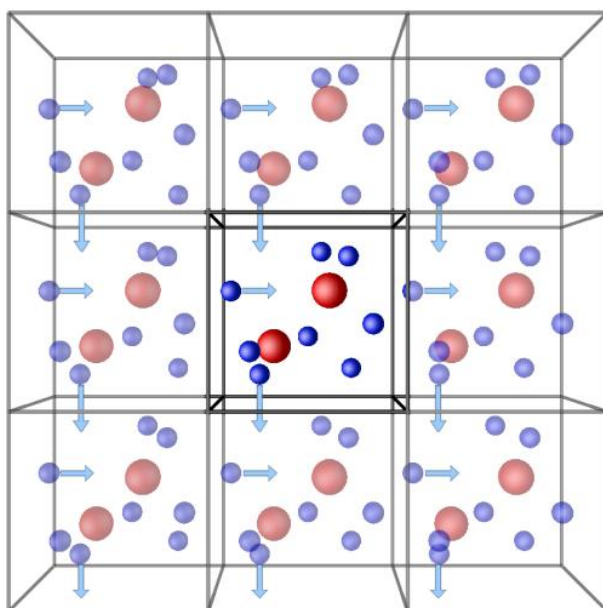
Figure 2 – Periodic boundary conditions. The central box with the molecule of interest (red), filled with water (blue), is replicated in copies of itself.

2.2.4 Potential Energy Minimization

The Potential Energy Surface (PES) is a complex multi-dimensional function of molecular system coordinates. PES is characterized by stationary point, minima and maximum. Minimum can be local or global, which corresponds to the lower energy, and represent the stable conformational states of the system. Algorithm permits to find the local minimum closest to the starting point and to reach the minimum energy of the system. Minimum are separated by high energy barrier, once the system is in a minimum requires high energy to overcome a maximum and reach another minimum.

Algorithm can act with two different methods: derivative and non-derivative. The first order derivative method change atom coordinates moving to lower energies and the starting point for each interaction is directly derived by the previous one (e.g., Steepest Descent[7] and Conjugate Gradient[8]). The second order derivative provide information about the curvature of the function and calculate the inverse Hessian matrix of second derivatives (e.g., Newton-Raphson and L_BFGS).

Energy minimization is widely performed before a molecular dynamics simulation, especially when the system is complex.

2.3 Molecular Dynamics

Molecular Dynamics (MD) is a computational approach used to calculate average properties of a system by sampling microstate. It is a deterministic method because the future state is completely determinate from the present state. MD is used to compute equilibrium and transport properties solving Newton's equation through a potential energy function, the force field.

2.3.1 Statistical ensemble

There are two categories of macroscopic properties in a chemical system: static equilibrium properties (e.g., temperature, density, pressure) and dynamic or non-equilibrium properties (e.g., diffusion process, dynamics of phase change). A representative *statistical ensemble* is defined to compute macroscopic properties. The *phase space* contains all the possible states that the system can reach, it often consists of all possible values of position and momentum variables. A single point in phase space describes the state of the system and the succession of this plotted points represents all the accessible system's microstates. There are different points I the phase space characterized by the same thermodynamic state. The collection of all

possible system configurations which have different microscopic states, but an identical thermodynamic state is known as *statistical ensemble*. There are different ensembles:

- o The Canonical ensemble (NVE) corresponds to an isolated system, it is characterized by fixed volume (V), energy (E) and number of atoms (N);
- o The Isothermal-Isobaric ensemble (NVT) corresponds to a closed system where number of atom (N), volume (V) and temperature (T) are kept constant;
- o The Gran Canonical ensemble (μVT) corresponds to an open system and the fixed characteristics are temperature (T), volume (V) and chemical potential (μ);
- o The Microcanonical ensemble (NPT) maintain constant number of atoms (N), temperature (T) and pressure (P).

The ensemble average of property A is determined by integrating over all possible configuration of the system by:

$$< A >= \iint A(p^N, r^N)\rho(p^N, r^N)dp^N dr^N$$

Where $A(p^N, r^N)$ is the observable of interest, r is the atomic position and p the momenta. The probability density function $\rho(p^N, r^N)$ of the ensemble is given by:

$$\rho(p^N, r^N) = \frac{1}{Q} \exp\left[\frac{-H(p^N, r^N)}{k_B T}\right]$$

where k_B is the Boltzmann factor, T is the temperature and H is the Hamiltonian. Q is an expression called partition function, that is a dimensionless normalizing sum of Boltzmann factor over all microstates of the system:

$$Q = \iint exp\left[\frac{-H(p^N, r^N)}{k_B T}\right] dp^N dr^N$$

Starting from the partition function lots of thermodynamics properties can be calculated. However, it difficult to solve analytically. To obviate this problem the ergodic hypothesis is used: over long periods of time, the time-average of a certain physical property, represents the ensemble-average of the same property.

$$< A >_{ensemble} = < A >_{time}$$

The time-average $< A >_{time}$ can be computed by:

$$< A >_{time} = \lim_{\tau \to \infty} \int_{t=0}^{\tau} A\big(p^N(t), r^N(t)\big) dt \ \sim \frac{1}{M} \sum_{t=1}^{M} A(p^N, r^N)$$

where t is the simulation time, M is the number of steps and $A(p^N, r^N)$ is the instantaneous value of the calculated property.

2.3.2 Molecular Dynamics Implementation Scheme

The central idea of MD is to solve Newton's equation of motion for a system of N interacting atoms (or particles). For each atom the acceleration is given as the derivative of the potential energy with respect to the position r:

$$a = -\frac{1}{m}\frac{dV}{dr}$$

The potential energy is a function of the atomic positions (3N) of all atoms in the system. This function is complex and is not possible to solve it analytically. Therefore, this equation is solved using some numerical integration scheme. The choice of the integration time-step is very important to avoid instability and to sample correctly the phase-space, usually the time-step is in fs. There are different integration methods for MD, for example a variation of the Verlet algorithm, called the Leap Frog Algorithm.

The process of a MD simulation can be simply explained with a flow chart (figure). The initial atomic positions are known (e.g., from Protein Data Bank) and initial atoms velocity v are randomly chosen from a Maxwell-Boltzmann distribution at a given temperature. The set of atoms coordinates, and velocities is generated step-by-step, giving the trajectory that describes positions, velocities and accelerations of the particles as a function of time. The MD method is deterministic: once the position and velocities of each atoms are known, the state of the system can be predicted at any time in the future or in the past. After initial changes, the molecular system reaches an equilibrium state: this can be interpreted as a statistical ensemble that will provide a macroscopic description of the behaviour of the system. Using the output trajectory of the MD, the macroscopic thermodynamic properties can be calculated as time averages.
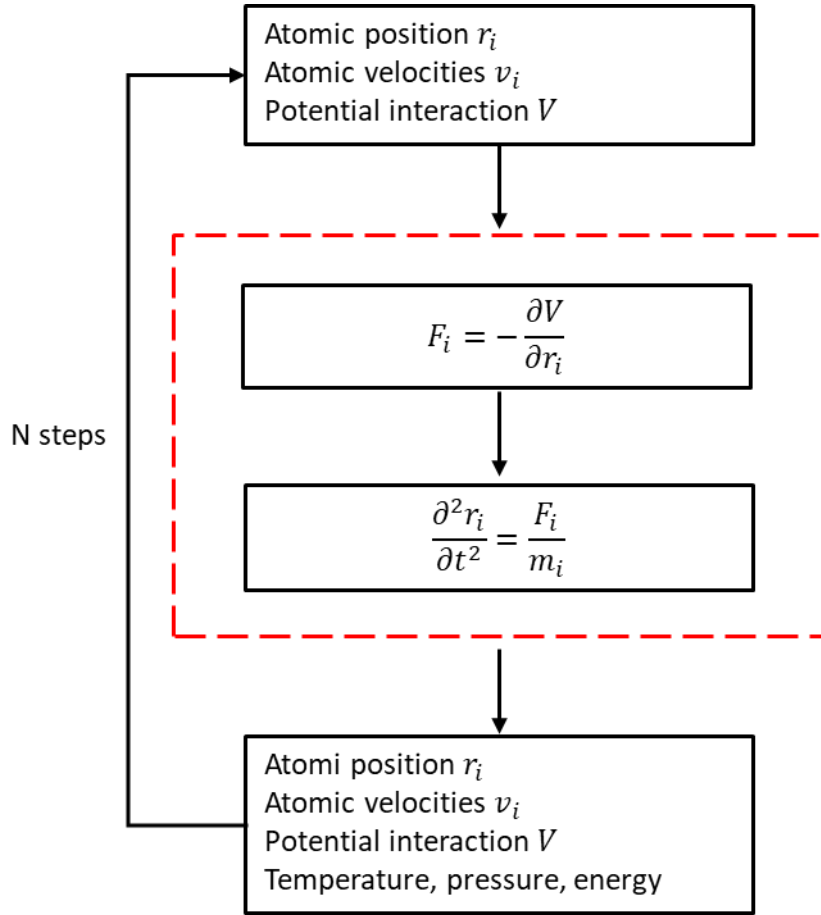
Figure 3 - MD flow chart. The initial atomic position and velocities are known. The potential energy V is calculated from the atomic position r_i. The process continues with the calculation of the forces F_i acting on each atom deriving the potential energy function. From the integration of the equation of motion, new position r_i and new velocities v_i are calculated. The cycle goes on for a number of steps until the equilibrium is reached (convergence of the computed equilibrium property).

2.4 Membrane mechanics

Lipid bilayers are fundamental in cell life as they support the cell during its principal activities as cell division and endocytosis. Study the elastic properties of the cell membrane is useful to better understand these phenomena. An important contribution in this compound is the one given by Helfrich[9], which models the plasmatic membrane as a thin, structureless and homogeneous fluid sheet. Lipid bilayers' mechanical properties are described by the bending modulus K_C, which represent the energy necessary to induce a deformation, applying a stress, starting from the local curvature, and the effective spontaneous curvature C_0, which describes the preferred curvature of the interface. These properties are influenced by characteristics of the environment (e.g., temperature, pH), different type of lipids, and the presence of components (e.g., transmembrane proteins, nanoparticles).

Bending modulus can be calculated in different ways, such as techniques based on the analysis of thermal fluctuations of large membranes; techniques based on the application of a stress to bend the membrane using, for example, micropipettes or optical pliers; computational approaches based on molecular dynamics simulations; techniques based on X-ray and/or neutron scattering.

The bending modulus is used to describe the energy necessary to deform a bilayer from its intrinsic curvature. The bending energy per area can be calculated with the following equation:

$$E_{bending} = \frac{1}{2} K_C \left(\frac{c_1 + c_2}{2}\right)^2$$

where K_C is the bending modulus and c_1 and c_2 the principal curvatures[10] (Figure 4). The intrinsic membrane's curvature is considered zero.
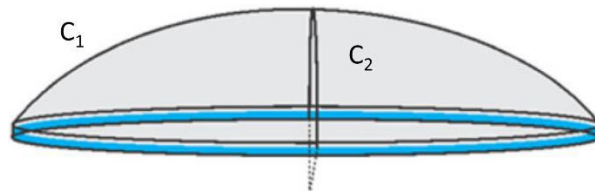

Figure 4 - Schematic representation of squared averaged curvature, where c_1 and c_2 are the principal curvatures.

2.4.1 Method based on thermal fluctuation

This approach provides the application of thermally excited fluctuations in the bilayer interface shape $u(x, y)$ of a pure lipid membrane through flicker spectroscopy[11] or in the course of a MD trajectory. According to Helfrich continuum description[9], bilayer deformations causes energy loss expanded to lower order terms in $u(x, y)$. The analysis of the banding rigidity is performed in Fourier space terms using the two-dimensional reciprocal space vector $\vec{q}$. Starting from the equipartition theorem is possible to calculate the bending modulus, in fact, the spectral amplitude profile $\langle u^2(q) \rangle$ for the small-q modes is:

$$\langle u^2(q) \rangle = \frac{k_B T}{A_{Box}} K_C q^{-4}$$

where A_{Box} is the lateral area of the simulation box, T the temperature and k_B the Boltzmann factor[12,13]. Using this method in MD simulation[14] is not simple because it requires membrane

containing at least 1000 lipids and the membrane dimensions has to be more than 20 nm to observe the bilayer fluctuations.

In case of smaller membrane, the study of membrane undulations can be change with the study of the fluctuations in lipid tilt, as proposed by Watson et al.[15]

2.4.2 Method based on applying a stress

Another theory can be used to calculate the bending module considering the lipid membrane composed by two uncoupled layers of d/2 thickness each:

$$K_C = \frac{Ed^2}{24(1 - v^2)}$$

Where E is the Young's module and v is the Poisson ration[16,17]. This equation is used in experimental techniques, as atomic force microscopy, where the Young's module is measured in small section of the membrane obtaining a local value for the elastic module instead of value for an entire lipid membrane or vesicle[18].

2.4.3 Method based on tilt/splay angle fluctuations

The bending modulus can be also obtained analysing fluctuations in lipid splay and tilt from molecular simulations[19,20].

The bending modulus is correlated with the ability of the lipid membrane component to change orientation respect the membrane normal, i.e., tilt angle, or respect each other, i.e. splay angle[21]. From molecular simulations both tilt module (χ) and splay module (χ_{12}) can be calculated, considering the free energy cost used to transfer a lipid from the aqueous medium into a lipid mixture bilayer at a specific angle. Both angles are defined in the range [0°; 90°]. The potential mean force ($PMF(\theta)$) is obtained from the probability distribution $P(\theta)$ of the tilt and splay angle:

$$PMF(\theta) = -k_B T ln \left[\frac{P(\theta)}{P_0(\theta)} \right]$$

where $P_0(\theta) = \sin(\theta)$ is the probability distribution of a hypothetical non-interacting particle system[19], k_B is the factor of Boltzmann and T is the temperature of the system. Fitting the $PMF(\theta)$ data with a quadratic function permits to obtain the tilt module χ and the splay module χ_{12}. Then the bending module of the monolayer can be calculated as weighted average:

$$\frac{1}{k_m} = \frac{1}{\phi_{total}} \sum_{\langle i,j \rangle} \frac{\phi_{ij}}{\chi_{12}^{ij}}$$

Where χ_{12}^{ij} is the splay modulus for the *ijth* pair type, ϕ_{ij} is the number of near-neighbouring *ij* encounter pairs, obtained directly from MD trajectories, and $\phi_{total} = \sum_{ij} \phi_{ij}$ represents the total number of encounters in the simulation for all possible pairwise contributions $\langle i, j \rangle$ for which the splay is calculated. Using the heuristic approximation, the bilayer bending module is:

$$K_C = 2k_m$$

Chapter 3

BIOLOGICAL BACKGROUND

Abstract

Alzheimer's disease (AD) is the most common form of dementia and is characterized by an irreversible loss of neurons. Inheritance excluded, age is the principal risk factor in dementia onset and because of the improvement of the quality of life the number of AD patients is increasing. Actually, there is not a cure and treatments available are not able to slow the pathology onset. The mechanism by which AD develops is still unclear. One of the most accredited hypotheses is the amyloid cascade, where aggregation of amyloid β (Aβ) peptide into plaques is considered the main cause in AD onset. There are two principal variants of Aβ peptide: $A\beta_{40}$, that is the most abundant, and $A\beta_{42}$, that is the most stable and toxic. An important aspect in the cascade hypothesis is the interaction between Aβ assembly with cell membrane, small aggregates seem to have deleterious effects on neuronal activities. In particular, a deepening of the effects of amyloid β peptide on cell membrane is made.

3.1   Introduction

Alzheimer's disease (AD) is a neurodegenerative disease that cause irreversible loss of neurons, principally in the cortex and hippocampus. AD is the most common form of dementia. With the progression of the pathology different symptoms arise, as impairment in memory, judgment, decision making, orientation to physical surroundings, and language[22]. Dementia is one of the expensive conditions to the society[23], in 2018, in United States, $277 billion have been spent for all people with AD or other forms of dementia[24].

In 2018, approximately 5.7 million Americans lived with AD, where new cases in people are 65 or older were 484,000, this number is going to double in 2050[25]. AD's principal cause is age and the probability of AD onset increase with age. Cases of AD in people younger than 65 are only related to inheritance[24]. Following the diagnosis life expectancy are between 3 and 9 years, however, in some cases, life expectancy reaches 20 years[26]. More women than men develop AD, two-thirds of Americans AD patients are women, this is probably due to the fact that women live longer than men. However, women life expectancy is greater than the one in men because they tend to survive longer in the severe stage[27].

Besides age, that is the principal risk factor in dementia onset, there are other factors that can be controlled (e.g., cardiovascular risk factor and psychosocial factors). Conducing a healthy life, excluding smoke, moderate alcohol consumption, and doing regular physical activities are useful to reduce the risk of AD onset[26]. Other studies demonstrate that people with a greater educational background show a reduced risk in AD development[28,29]. Accordingly, to avoid AD onset or to delay its development, it is advisable to consider these factors since young adulthood or middle age.

Established the exact number of deaths for AD is not simple, because dementia is rarely considered as the principal cause of death[30]. In facts, wallowing disorders, immobility and malnutrition are the principal consequences of acute dementia and can lead to death, pneumonia and other respiratory system disease are principal causes of earlier death in AD patient[31,32].

Diagnose AD is not simple because there is not a single test. Physicians use a variety of approaches to make a diagnosis, e.g., studying the individual family history, doing cognitive tests and physical and neurologic examinations, blood tests and brain imaging. Brain imaging is fundamental to find the presence of the two principal AD hallmarks: beta-amyloid plaques and tau tangles[24] (Figure 5). The former are intraneural aggregates of hyperphosphorylated tau proteins, the latter are extracellular plaques originated by the deposition of amyloid β (Aβ) peptide[33].
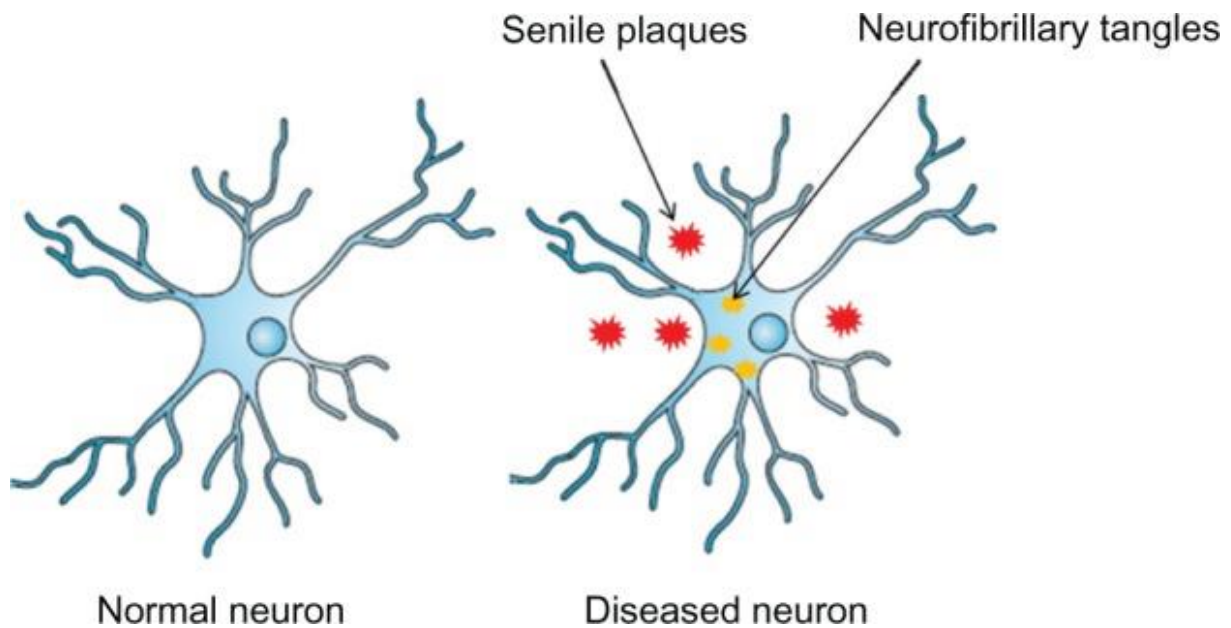
Figure 5 – Differences between a normal neuron and a neuron of AD patient. The two principal AD hallmarks are amyloid β plaques, which originates senile plaques, and hyperphosphorylated tau protein, which forms neurofibrillary tangles.

Actually, there are not treatments able to slow or stop damage or loss of neurons. The only six drugs approved by the U.S. Food and Drug Administration improve symptoms increasing the quantity of neurotransmitter in the brain. Contemporarily, AD patients are submitted to non-pharmacological treatments with the purpose to maintain or improve cognitive function and the ability to perform routine activities, and to reducing symptoms as agitation and depression. In particular, it is demonstrate that the combination of aerobic and non-aerobic exercises positively influences cognitive functions[34].

Since AD development is influenced by several factors, the mechanism of AD onset is still unclear. From the discovery of AD in 1906[35] scientists try to explain the mechanism behind this pathology. There are three principal hypothesis: cholinergic hypothesis[36], tau hypothesis[37], amyloid cascade hypothesis[38], and vascular hypothesys[39], recently developed.

3.1.1 Cholinergic hypothesis

This oldest hypothesis considers the cholinergic disfunction as the principal cause of AD onset. A reduction of choline acetyltransferase and acetylcholinesterase activity are found in cerebral cortex and other brain areas of AD patients[36] and *in vitro* studies confirms this hypothesis demonstrating that in first steps of AD development there is a selective degeneration of acetylcholine-releasing neurons. Cholinergic neurons play an important role

in cognitive functions, therefore their damage affects the developments of this disorder especially with regards to memory loss.

Since this event has been demonstrated and understood, different therapeutic approaches have been developed, including cholinesterase inhibitors and choline precursor. Actually, second generation inhibitors, characterized by longer half-lives, greater efficiency and less side effects, are used to treat these symptoms reaching beneficial effect[40].
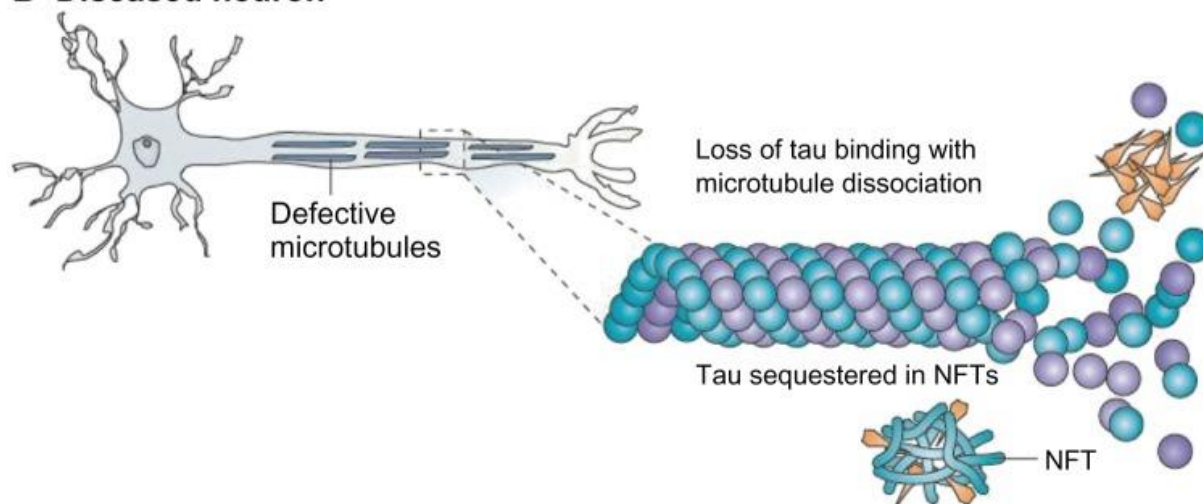
3.1.2 Tau hypothesis

Tau proteins are part of the family of microtubule associated proteins. They are fundamental in microtubule assembly and stabilization. In case of disease, the hyperphosphorylation causes a decrease capability of tau protein to bind microtubules and the sequestration of hyperphosphorylated tau protein into neurofibrillary tangles (NFT) (Figure 6). Besides, the abnormal deposition of hyperphosphorylated tau protein is found not only in neurofibrillary tangles but also in cytosol of AD brain. A loss in normal tau function influences normal cellular functions as maintenance of appropriate morphology, axonal transport, synaptic dysfunction and neurodegeneration[41].
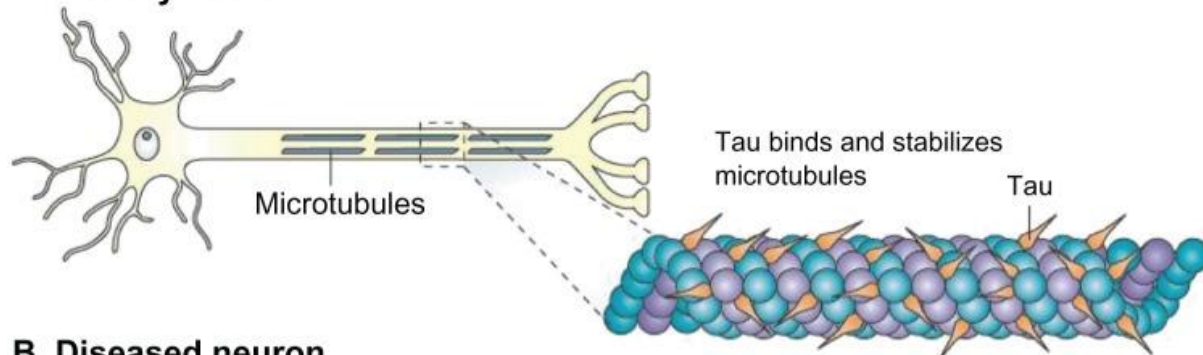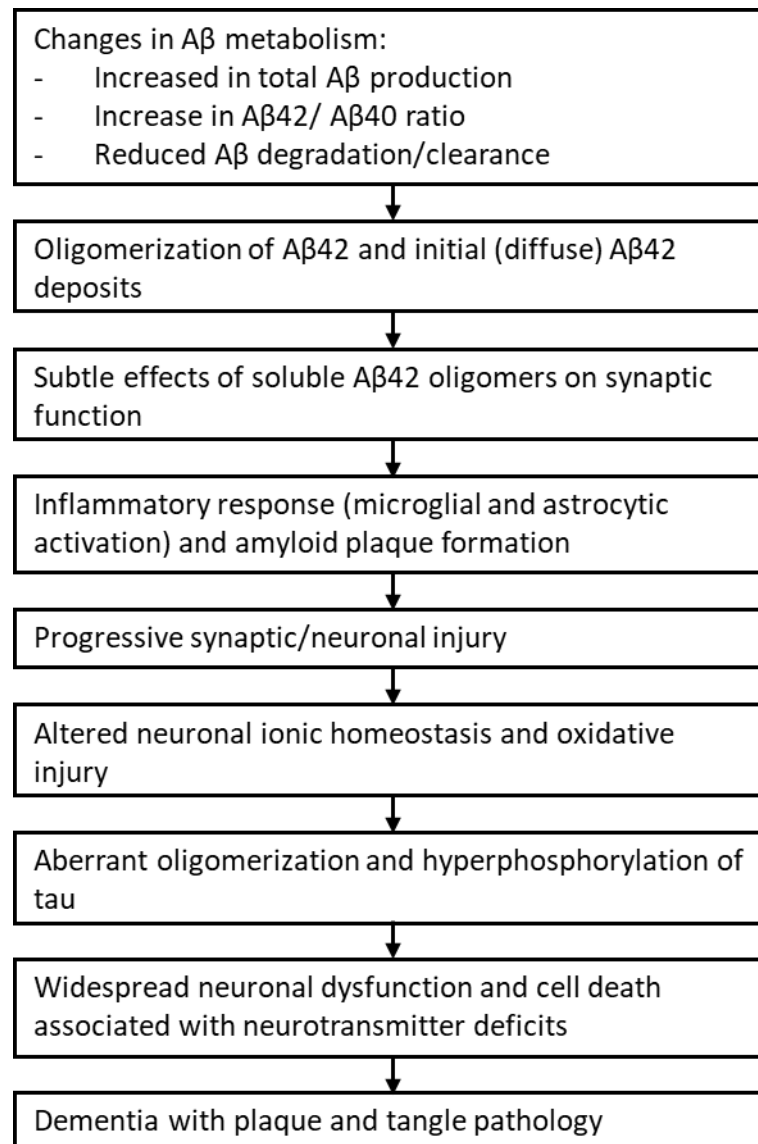
Figure 6 – Representation of tau hypothesis. Tau proteins are fundamental in microtubule assembly and stabilization. Their hyperphosphorylation cause the sequestration in neurofibrillary tangles (NFTs). A loss in normal tau function influences cell activities such as maintenance of appropriate morphology, axonal transport, synaptic dysfunction and neurodegeneration.

3.1.3 Amyloid cascade hypothesis

Nowadays, the most accredited hypothesis consider the abnormal accumulation of beta-amyloid plaques in various areas of the brain as the principal cause of AD onset, and neurofibrillary tangles, cell loss, vascular damage and dementia as the consequences of the deposition[38].

The amyloid cascade (Figure 7) starts with changes in Aβ protein level in brain. The increase in Aβ peptide concentration is due to an enhanced production and/or reduced clearance. Mutation on genes APP, PS1 or PS2 influences the metabolism or stability of Aβ peptide, e.g. a mutation on PS1 increase the level of $A\beta_{42}$ peptide leading to its accumulation[42]. $A\beta_{42}$ accumulation increases oligomer formation, which is responsible to changes in synaptic function. At the same time, there is a formation of amyloid plaques by $A\beta_{42}$. Plaques act as

deposits of Aβ peptide, causing an inflammatory response. These events involve oxidative stress and altered ionic homeostasis. Changes in kinase and phosphatase activities embroil neurofibrillary tangles that contributes to other defects. The culmination in cascade is reached with diffused synaptic/neuronal disfunction and cell death, leading to a progressive dementia[43].

Changes in Aβ metabolism:
- Increased in total Aβ production
- Increase in Aβ42/ Aβ40 ratio
- Reduced Aβ degradation/clearance

↓

Oligomerization of Aβ42 and initial (diffuse) Aβ42 deposits

↓

Subtle effects of soluble Aβ42 oligomers on synaptic function

↓

Inflammatory response (microglial and astrocytic activation) and amyloid plaque formation

↓

Progressive synaptic/neuronal injury

↓

Altered neuronal ionic homeostasis and oxidative injury

↓

Aberrant oligomerization and hyperphosphorylation of tau

↓

Widespread neuronal dysfunction and cell death associated with neurotransmitter deficits

↓

Dementia with plaque and tangle pathology

Figure 7 – Amyloid cascade hypothesis. Changes in Aβ metabolism lead to the deposition of Aβ$_{42}$ soluble oligomers, which influences synaptic functions. Subsequently synaptic and neuronal injuries are consequences of the activation of the inflammatory response and the amyloid plaque formation. Alterations in neuronal activities and hyperphosphorylation of tau protein leads to neuronal disfunction, irreversibly cell loss and progressive dementia onset.

3.1.4 Vascular hypothesis

This hypothesis has been developed recently and is based on reduced cerebral blood flow, glucose metabolism and oxygen utilization observed in patients with AD.

Neurodegeneration is the main cause of AD onset. With advancing age vascular risks factor develop leading to a chronic brain hypoperfusion (CBH) and critical attained threshold of cerebral hypoperfusion (CATCH). Oxidative stress and neuronal energy crisis are the direct consequences of CATCH and involve energy decline. Moreover, the chronical ischemic-hypoxic state leads to the aggregation of amyloid β protein. Consequently, the minor availability of the protease responsible for Aβ peptide cleavage cause the abnormal deposition of Aβ plaques and to the AD onset[44].
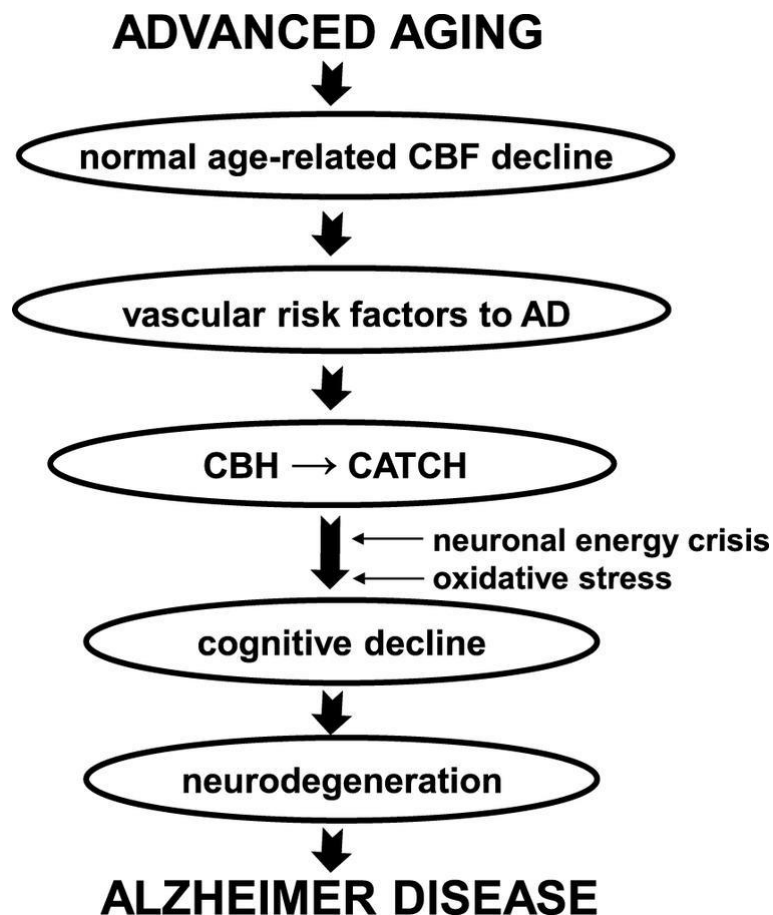

Figure 8 - Vascular hypothesis. With advancing age vascular risks factor develop leading to a chronic brain hypoperfusion (CBH) and critical attained threshold of cerebral hypoperfusion (CATCH). Oxidative stress and neuronal energy crisis are the direct consequences of CATCH and involve energy decline. Consequently, the minor availability of the protease responsible for Aβ peptide cleavage cause the abnormal deposition of Aβ plaques and to the AD onset.

3.2 Amyloid β protein

Despite different hypotheses have been developed to explain AD onset, Amyloid β peptide aggregation into plaques is considered one of the leading causes of cell death and memory loss.

Aβ peptide was firstly isolated in 1984[45]. Aβ peptide originates from an amyloid precursor protein (APP), by groups of enzymes: α-, β-, γ- secretase. APP is widely expressed in body cells and the amount produced is influenced by the development and the physiological state of the cells. The cleavage and processing of APP can be divided into a non-amyloidogenic pathway and an amyloidogenic pathway, that produces Aβ peptide[46] (Figure 9). The non-amyloidogenic pathway precludes Aβ formation and is the most processed. The α-secretase mediate the first cleavage, since it happens within the Aβ domain, there is no production and release of Aβ peptide. Thus, the two products are the ectodomain (sAPPα), which is the larger, and the carboxy-terminal fragment (C83). APP molecules that not undergo the non-amyloidogenic pathway are cleaved by β-secretase. This enzyme releases an ectodomain (sAPPβ) and preserves the last 99 amino acids of APP (C99). Since the first amino acid of C99 is the first amino acid of Aβ, when C99 is cleaved by γ-secretase Aβ peptide (with between 38 and 43 residues) is released. As γ-secretase is composed by PS1 or PS2, their mutation affects Aβ production.
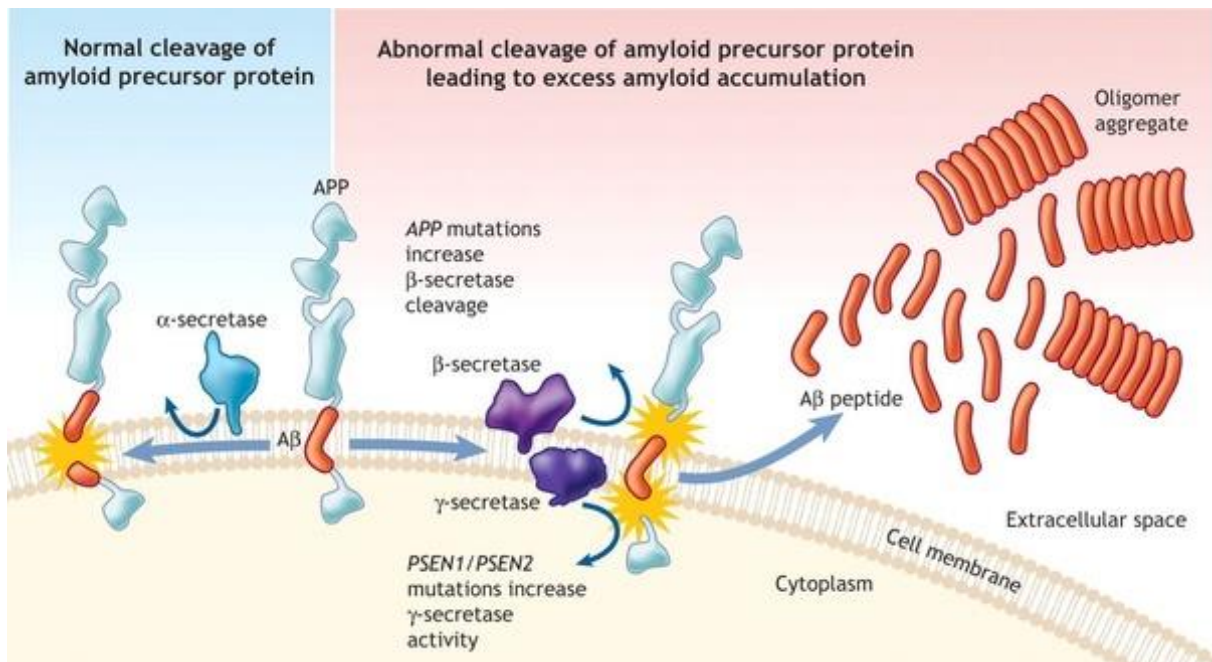
Figure 9 - Aβ peptide originated from an amyloid precursor protein (APP), by groups of enzymes: α-, β-, γ-secretase. The cleavage and processing of APP can be divided into a non-amyloidogenic pathway and an amyloidogenic pathway, that produces Aβ peptide. The non-amyloidogenic pathway precludes Aβ formation and is the most processed. The α-secretase mediate the first cleavage and there is not the production and the release of Aβ peptide. APP molecules that not undergo the non-amyloidogenic pathway are cleaved by β-secretase. This enzyme releases an ectodomain (sAPPβ) and preserves the last 99 amino acids of APP (C99). Since the first amino acid of C99 is the first amino acid of Aβ, when C99 is cleaved by γ-secretase Aβ peptide (with between 38 and 43 residues) is released.

In this process, the 90% of Aβ peptide produced is composed by 40 residues ($A\beta_{40}$), the remaining part is constituted by 42 residues ($A\beta_{42}$)[46]. $A\beta_{40}$ and $A\beta_{42}$ form oligomer and fibrils in various size starting from the monomer[47]. $A\beta_{40}$ is the more present in amyloid plaques and can assumes only a U-shaped form. $A\beta_{42}$ is less abundant but tends to aggregate more rapidly and represent a more toxic species. The two extra residues lead the protein to assumes both U- and S- shaped structure[48] (Figure 10). Recent studies demonstrate that S-shaped form is the most stable and compact specie[49].
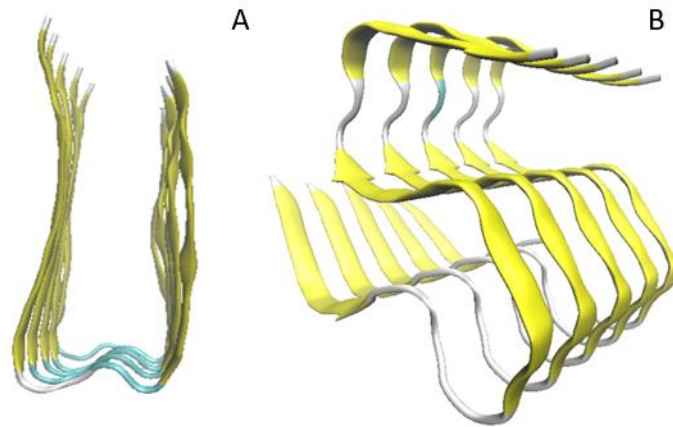
Figure 10 - Aβ$_{40}$ and Aβ$_{42}$ are the two principal forms of amyloid β peptide. The former can assume only U-shaped structure while the latter can assume both U- and S-shaped structure, thanks to the two extra residues.

Aβ peptides tend to aggregate into both ordered, originating fibre, and disordered, generating oligomer, assemblies. Aβ peptides are characterized by a longer ordered region (residues 10-40) and a shorter disordered region (residues 1-9), which leads to study the toxicity of the aggregates. By the way, neither of the two regions is toxic if taken individually. In particular, the ordered part influences how the peptide attaches to cell membrane and, once the aggregates fit into the cell, the N-terminal part interacts with an unknown cellular component. This interaction seems to deflect the aggregates toxicity pathway. Thus, both the regions play a fundamental role in AD onset.

Amyloid assemblies can be distinguished into three principal groups: monomers, soluble oligomers and fibrils, which contain different structure based on different organisation. It appears that the toxicity is linked to the size of the aggregate, in particular, as the size increase, the level of toxicity decreases (Figure 11). Despite the dimer is considered the most toxic oligomer, this presence is not detected during animal tests. This happen because oligomers can form a secondary nucleation reaching Aβ*56 assembly.
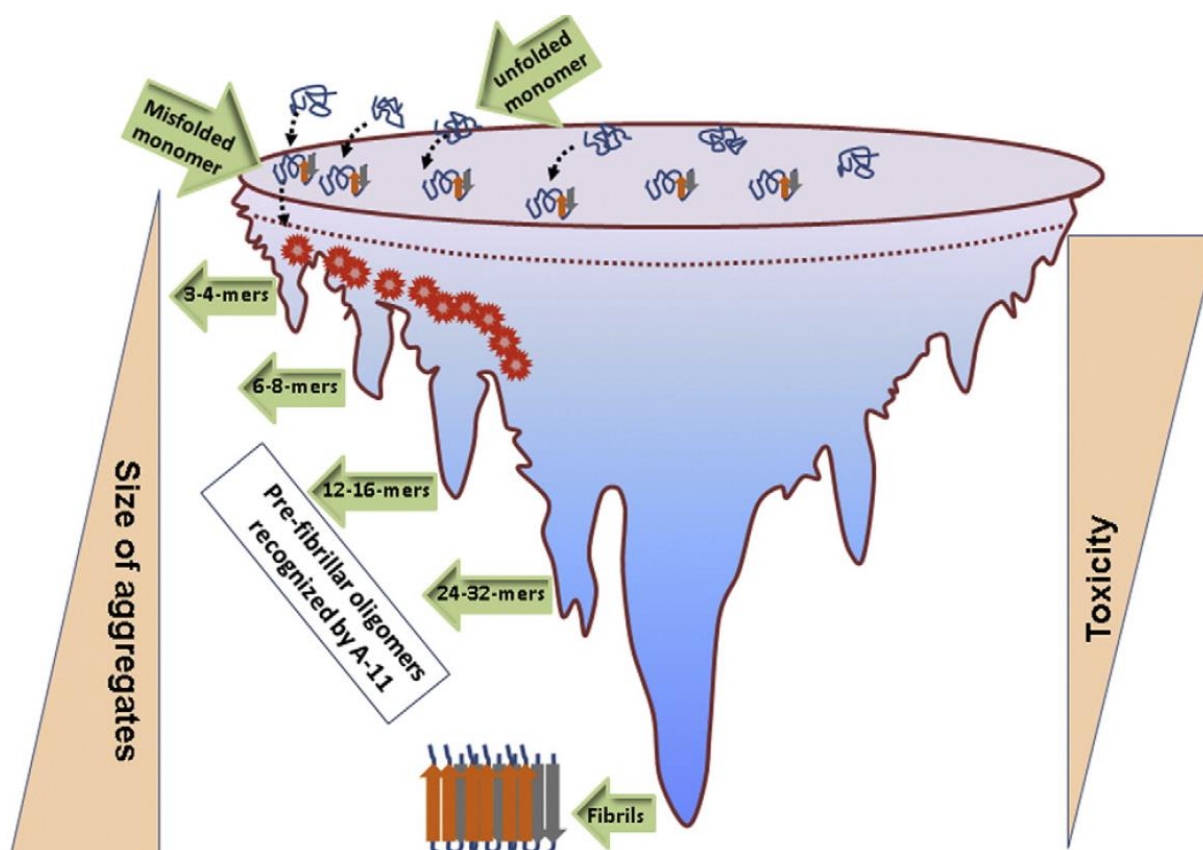
Figure 11 - Amyloid peptides tend to aggregate originating fibres and oligomers. The toxicity is linked to the size of the aggregate, in particular, as the size increase, the level of toxicity decreases.

Oligomers are characterised by a structural instability. Information about secondary structure are fundamental in development of therapeutic treatments. Aggregates can be distinguished in different structural classes; two of them (fibrillar oligomers, FOs, and prefibrillar oligomers, PFOs) have been studied in an experimental work[50]. The secondary structure of FOs is mainly β-sheet, while the one of PFOs is more disordered. Various techniques have been used to analyse the secondary structure. They found that FOs are similar to fibrils but less stable unlike PFOs are much less ordered.

Interestingly, the interaction between Aβ40 and Aβ42 leads to the formation of smaller, more stable and more toxic structure[51]. The produced aggregates have different characteristics base on the ratio between the quantities of the two conformations.

3.2.1 Amyloid peptide fibrilization

Plaque formation is observed as a consequence of the fibrillization process of the amyloid peptide. As previously mentioned, Aβ42 peptides tend to form plaques faster than Aβ40. This difference is probably due to the two additional hydrophobic residues.

Fibrillogenesis occurs according to different mechanism. However, the tendency to form fibres is a common feature of peptides and proteins, especially in some conditions, e.g. denaturation[52]. Inter- and intramolecular forces are fundamental in fibrils stabilization; in particular, the amyloidogenicity is influenced by hydrophobicity and net charge[53]. Inter- and intramolecular forces modulate also the protein interaction with cellular membrane.

Once the peptide is produced by APP secretase it is subjected to elution inside the membrane and then the fibrils formation process is observed. This last step influences the lipid bilayer fluidity leading to its disruption. In a recent experimental work[54], a possible fibrilization pathway is proposed, investigating how the cellular membrane is involved in this process. The two *in vitro* models prepared differ in the way in which the protein comes into contact with the membrane. In one case the monomer is added to a preformed bilayer, external addition, while in the other case, the monomer is inserted into lipid micelles, pre-incorporation procedure. In case of external addition, the formation of the fibre is observed (Figure 12). After the deposition of the peptide on the bilayer surface, the fibril seed is formed, and the fibril elongation is observed. In this work, it is also proposed a method able to block the fibrils formation avoiding the deposition of the fibril seed. In fact, in presence of an agent capable of blocking the initial state of fibrillation, the peptides remain agglomerated at the intermediate structure characterized by a lower degree of toxicity than that of the fibre.
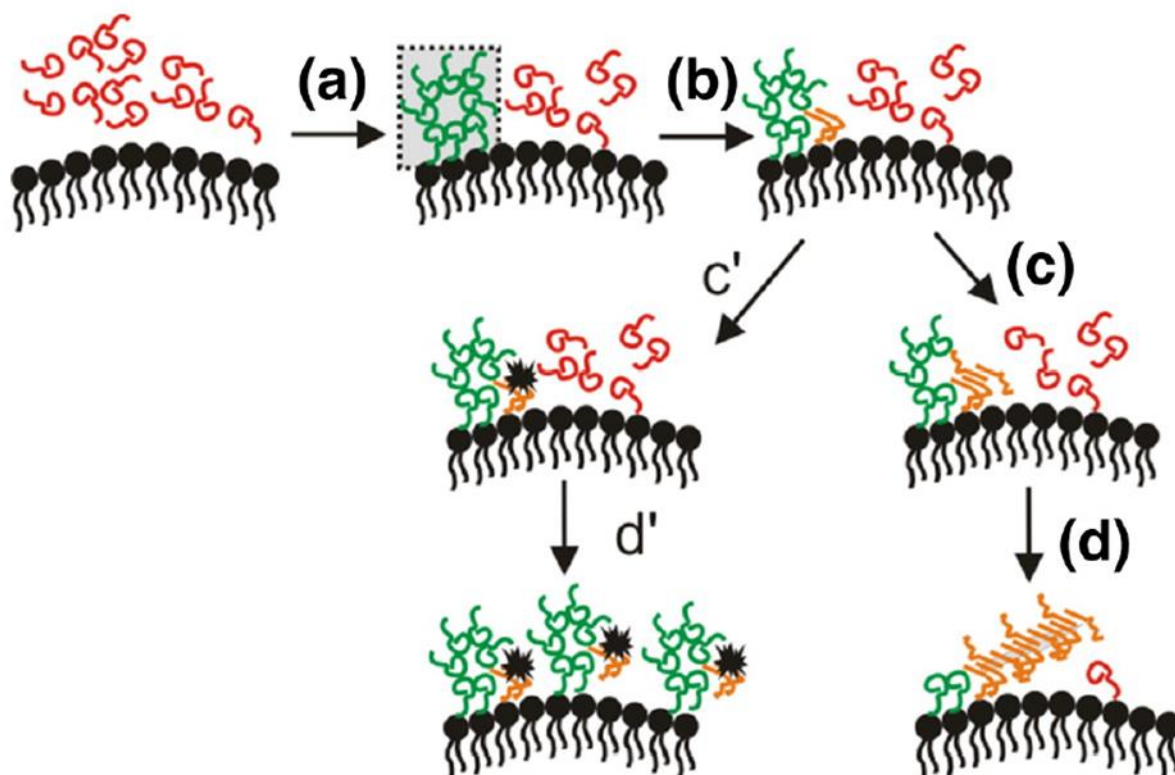
Figure 12 – Representation of the amyloid peptide fibrilization. After the deposition of the peptide on the bilayer surface, the fibril seed is formed, and the fibril elongation is observed. In presence of an agent capable of blocking the initial state of fibrillation, the peptides remain agglomerated at the intermediate structure characterized by a lower degree of toxicity than that of the fibre.

3.2.2 Aβ function

Despite the high toxicity, the Aβ peptide has positive roles in some physiological process, such as neurogenesis, synaptic plasticity and memory formation, and metal sequestration and antioxidant activity[55].

As regards the neurogenesis, the neuronal stem cells (NSCs) proliferation and neurogenesis are favoured by the Aβ$_{40}$ peptide, while the Aβ$_{42}$ protein encourages NSCs gliogenesis. Amyloid peptides have neuroprotective effects and enhance the cell viability in absence of growth factors. Autophagy is a process by which the Aβ peptide influences the neurogenesis. Low concentrations of soluble peptide increase the autophagy leading to the differentiation of the NSCs in a ROS-independent manner. This process seems to cause a survival response from the NSCs[56].

The synaptic plasticity is the ability of the nervous system to modify the intensity of intraneuronal synapses, to establish new ones and to eliminate some of them. It is fundamental in learning and memory formation[57]. During AD developments, synaptic plasticity and long-term potentiation, which concerns long-term memory, decrease whit the deposition of amyloid plaques. However, micromolar concentration of amyloid protein seems to favour the memory formation while the inhibition of the endogenous Aβ peptide production seems to reduce the memory retention[58,59].

The participation of metals such as zinc and copper in biochemical redox reactions produces the reactive oxygen species. If present in low concentration, the amyloid peptide tends to reduce this consequence because the histidine residues bind to metal ions preventing their participation in the redox reactions[60,61]. A study has confirmed the antioxidant ability of the amyloid protein in a cell-free system[62].

3.3 Interaction with the cell membrane

The amyloid protein interaction with cellular membrane is considered one of the principal mechanisms in Alzheimer's disease onset. In fact, the association and the interaction of amyloid oligomers with the cell membrane produces toxic effects on the normal cell functions and activities. Interactions between Aβ protein and cell membrane are crucial in AD onset, to better understand causes of AD is fundamental to investigate this mechanism. Experimental techniques currently used do not allow an atomic resolution, so computational approaches are necessary to study this microscale mechanism. In particular, MD simulations are used to clarify conformation of Aβ peptide and its aggregates in presence of cell membrane, imitate the adsorption process of Aβ peptide into the membrane surface, explain peptide assembly and the consequences on membrane deformation[63].

Amyloid-membrane interactions can be analysed from a double viewpoint as, on one hand, the lipid bilayer influences peptide misfolding and aggregation, and, on the other hand, peptide aggregates modify membrane integrity and permeability. Moreover, amyloid peptides used the cellular membrane ad an extensive surface during process of aggregation and fibrillization, while the membrane screens the cytosol from the interactions with amyloid aggregates. Interestingly, amyloid protein seems to have preferences for certain lipids domains or cell receptors.

Aβ peptide interacts with cell membrane in three different ways, depending on the peptide-to-lipid ratio, which lead to the bilayer disruption (Figure 13)[64]:

o Carpeting on the surface[64]

o Generating transmembrane oligomeric pores, causing non-specific ions permeation[65,66]

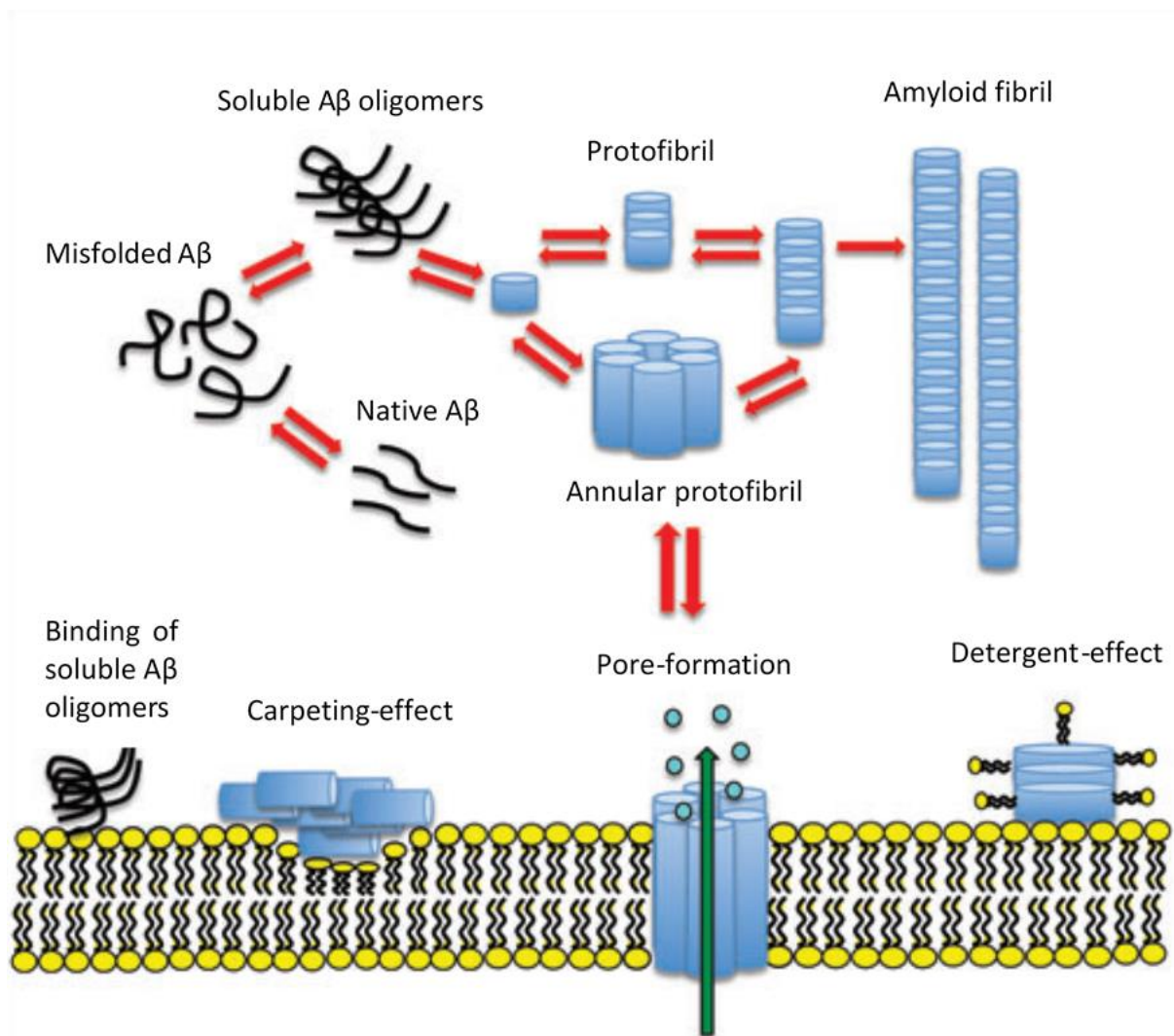o Accumulating on membrane surface causing detergent-like membrane dissolution[67]

Figure 13 - Aβ peptide interacts with cell membrane in three different ways, depending on the peptide-to-lipid ratio, which lead to the bilayer disruption: carpeting on the surface, generating transmembrane oligomeric pores, and accumulating on the membrane causing its detergent-like dissolution.

The carpeting process is not the principal cause of amyloid toxicity as damages lipid membrane at the same way as other protein[68]. However, it is probably related to the kinetics dissipation. Principal consequences of the protein carpeting on one bilayer leaflet is the asymmetric pressure between the two leaflets and the dispersion of small molecules[69].

The formation of ions channel is considered one of the principal toxic effects in AD onset. In particular, the hyperphosphorylation of tau protein an death cell are related with the variation in Ca^{2+} homeostasis[38]. It is proved that the insertion of $A\beta_{40}$ into a planar lipid bilayer forms pores that established linear current-voltage relationships in formal solutions[70]. Also, computational simulations observe ion channel formation. In particular, it is proposed that the most stable transmembrane pore originated between six hexamers[71]. However, also the subdivision of an octamer into two tetramers seems to generate an ion channel[72].

The third model of the interaction between amyloid peptide and cellular membrane is the detergent-like dissolution due to the peptide formation on a bilayer leaflet. In fact, during peptide formation, lipids tend to associate with the protein into micelle-like structure. The direct consequence of high concentrations of amyloid proteins, in the monomer or oligomer form, on the cell surface or of interaction between assemblies and lipids is a change in membrane permeation[73]. Initially, electrostatics forces drive the interactions between protein and lipid headgroups or between assembly and receptors on the membrane surface. Consequently, the peptide rotates to place its hydrophilic surface in contact with lipids headgroups introducing itself into the bilayer. This lead to the membrane disruption due to changes in bilayer curvature[73]. Therefore, the detergent-like membrane have two different consequences based on how the protein interacts with the membrane, if the lipids of a single leaflet are removed then there is a decrease in bilayer thickness while if the lipids of both layers are removed there is a hole formation[69].

However, the process of destruction of the cell membrane cannot be associated with only one of these three mechanism but depends on their combination. In fact, each mechanism is associated with a different step in protein aggregation. The carpet and the detergent-like models come about the protein is in form of peptide or small oligomer while the pore formation happen when assemblies interact with specific receptor.

3.4   Aβ interactions with lipids

Phospholipids are constituted by two hydrophobic fatty acids bound to carbon atoms in the glycerol, joined to the hydrophobic headgroup with a negatively charged phosphate group. This gives the lipids the amphipathic character. Since, the first surface with which Aβ peptide comes into contact is the cell membrane, it is interesting to analyse the consequences of the interactions between Aβ protein and different types of lipids. Starting from this objective, different kinds of analysis are made using experimental techniques, e.g. fluorescence

spectroscopy, atomic force microscopy, and computational modelling, e.g. molecular dynamics.

To study the relationships between the aggregation of amyloid peptide and the cellular membrane, micelles consisting of a single type of neutral lipid are produced[74]. Interestingly, it is found that in presence of phosphatidylcholine vesicles there is an increase in time necessary to the peptide aggregation. Also, nucleation and elongation decrease when $A\beta_{40}$ peptides comes into contact with micelles. Another study[75] demonstrates that headgroups lipids charge influences the aggregates' secondary structure. In particular, when the protein is dissolved into hydrophobic solvent it assumes an α-helical structure, while when the peptide comes into contact with different types of lipids it assumes a β-sheet structure. Therefore, it can be seen that the lipids electrostatic charge affects the protein behaviour.

A comparison between 1-palmitoyl-2-oleoyl-sn-glycero-3-phosphocholine (POPC) and 1-palmitoyl-2-oleoyl-sn-glycero-3-phospho-rac-(1-glycerol) (POPG) bilayer showed that $A\beta_{40}$ peptide has greater affinity with POPG lipids[76]. In addition, POPG is characterized by a higher mass adsorption than POPC and increases the amyloid peptide aggregation[77].

The membrane's surface charge influences the binding capacity of the amyloid protein to the lipid bilayer surface. In fact, amyloid β proteins bind preferentially to a negatively charged surface. Although the electrostatics forces are fundamental in these interactions, also the hydrophobic forces have an important role principally in the interaction between amyloid fibrils and cellular membrane.

As reported in the previous paragraph, $A\beta_{42}$ aggregates interact with cellular membrane causing its detergent-like disruption and generating ions channel. Some experimental works study the effects of the interactions between amyloid aggregates and cellular membrane. in particular, in increase in membrane permeation is the direct consequence of the interaction between $A\beta_{42}$ oligomer with DOPC vescicle[78]. Instead, fibrils, formed from the aggregation of amyloid peptides, are characterized by a decreased tendency to modify the lipid bilayer permeation. However, when small oligomers come into contact with DOPC vesicles, they tend to elongate forming amyloid fibrils associated with the membrane. Therefore, the interaction of amyloid peptide with lipid bilayer to form fibrils causes the cellular membrane disruption[68]

Since current experimental techniques do not allow microscale resolution, various computational studies have been done to analyse the interaction of amyloid assemblies with

cellular membrane at atomic level. Also, in this case, different behaviours are found, basing on the type of lipid with which the protein interfaces. *Xu et al.*[79] compare the differences in Aβ pentamer adsorption on POPC and POPC/POPG bilayers. The protein tends to bind more strongly with the POPC/POPG bilayer, that is anionic, than with zwitterionic POPC bilayer because electrostatics forces improve the adsorption. Furthermore, anionic bilayer promotes strong Aβ-Aβ interactions unlike zwitterionic bilayer that encourage strong Aβ-lipid interactions[80]. Effects of the insertion of Aβ40 trimer into zwitterionic DOPC bilayer are studied with REMD simulations[81]. Thanks to intermolecular interactions between protein and lipids, the membrane remains stable during the entire simulation as the trimer, in fact its size remains unchanged both in solution and in membrane. Only fluctuations on the order parameter are observed. *Poojari et al.*[82], in their work, underline the stability of POPC bilayer during interactions with amyloid assembly, in fact, the protein secondary structure remain unaltered when inserted into the bilayer.

3.5   Aβ interactions with cholesterol

Cholesterol is a membrane lipid and is irreplaceable in the membrane of animal cells as influences membrane fluidity, permeability and dielectric properties. In fact, this lipid favours the phospholipids immobilization decreasing the membrane viscoelasticity and the passage of small water-soluble molecules. In brain of AD patient there is a decrease in the cholesterol to lipid ratio that can reach 33% less than brain of healthy person[83]. This means that the major cellular membrane fluidity favours the amyloid protein permeation. Moreover, a decrease cholesterol-lipid ratio is related to the bilayer thinning and then to a major exposure of APP sites which leads to an increase in amyloid peptide production[84]. Variations in cholesterol quantities are related with ageing and influences amyloid peptide degradation, as this process requires the activation of plasmin in cholesterol-rich domains[85].

Cholesterol content higher than 20% w/w causes the transition from a fluid-disordered bilayer to a fluid-ordered state, which make Aβ peptide permeation more difficult. Therefore, the cholesterol to phospholipid ratio influences the binding affinity of Aβ protein, that decrease in case of pure phospholipid membrane[86]. However, experimental studies[87,88] show conflicting opinions regarding the insertion of the amyloid protein into the membrane containing cholesterol. This is probably due to the fact that a non-phospholipids pure bilayer increases the binding affinity and, then, the interaction with the Aβ peptide. Thus, membrane rich in

cholesterol does not allow the fibril formation because it is characterized by a greater permeation of the protein inside it.

Also, computational studies focus on the consequences of the cholesterol presence in the lipid bilayer. Simulations of Aβ(11-42) fibre with POPC bilayer[89] show that assembly with more than two peptides tend to deform the bilayer and generate water channels, besides, increasing in assembly dimensions leads to a decreasing in free energy of penetration. Moreover, high concentration of cholesterol inside the bilayer seems to avoid the peptide penetration inside the bilayer.

Chapter 4

THE IMPACT OF AMYLOID BETA ASSEMBLY ON MEMBRANE CONFORMATIONAL STABILITY AND DYNAMICS

Abstract

One of the hypothesis of Alzheimer's disease onset is based on the amyloid cascade according to which the deposition of amyloid β (Aβ) peptide into plaques is responsible for neuronal injury and memory loss. Amyloid assemblies interact with cell membrane causing ionic homeostasis, membrane leakage and cell toxicity. Molecular dynamics (MD) simulations allow to study these influences at microscale level.

In this chapter $A\beta_{11\text{-}42}$ peptide, oligomer and fibre are inserted into POPC bilayer in order to analyse effects of mutual interaction. Results shows that proteins have the same behaviour both in water and in membrane. While, assemblies change the bilayer properties. Both oligomer and fibre influence at the same way the area per lipid and the bilayer thickness and differently the tilt and splay angles. In particular, order parameter and bending modulus show a dependency on the distance from the protein.

4.1   Introduction

Small assemblies of amyloid β peptide (Aβ) are considered the primary neurotoxic species that causes Alzheimer's disease (AD) and other neurodegenerative disorders (e.g., Huntington disease)[90]. The mechanism by which AD develops is not clear. Many hypotheses have been made to try to explain AD onset, as the cholinergic hypothesis, the tau hypothesis, the amyloid cascade hypothesis and the vascular hypothesis. The amyloid cascade is the most accredited hypothesis and consider the deposition of amyloid β plaques around neurons as the principal cause of the irreversible neuronal damage and memory loss. Aβ peptide is product from cleavage of the Amyloid Precursor Protein (APP) by α-, β- and γ-secretase[91]. There are two principal type of Aβ peptide, one constituted by 40 residues ($A\beta_{40}$), which accounts for 90% of secreted Aβ, and a less prevalent type constituted by 42 residues ($A\beta_{42}$)[92]. $A\beta_{42}$ is the most toxic specie and tends to aggregate more rapidly[93]. Aβ fibres are characterized by

polymorphism[94], Aβ_{40} can assume only a U-shaped structure instead of Aβ_{42} that can adopt both U- and S-shaped structure[95]. Recent studies demonstrate that the S-shaped Aβ_{42} is the most compact and stable specie[49]. Changes in Aβ metabolism lead to peptide deposition and aggregation. Small soluble oligomers generate inflammatory response and plaque deposition. Consequently, synaptic and neuronal injury, altered ionic homeostasis and hyperphosphorylation of tau protein are observed. These phenomena lead to neuronal dysfunction and dementia onset. Actually, there are no treatments able to slow down or stop the pathology, thus is fundamental a better comprehension of this mechanism.

Amyloid peptide tends to interact with cell membranes. The association and the interaction of amyloid oligomers with lipid bilayer produce toxic effects on the normal cell functions and activities. In fact, besides the interactions with the membrane receptors, amyloid peptides can adsorb on, insert to and destabilize cell membrane. Physical and direct interaction between the peptide and the membrane leads to the disruption of the cell membrane in different ways, e.g. carpeting on the surface, penetrating in the cell membrane causing transmembrane channels, causing detergent-like membrane dissolution. Ionic homeostasis, membrane leakage and cell toxicity are due to the disruption of the cell membrane, that causes the penetration of small molecules and ions inside the cell[96]. Changes in these interactions are due to the bilayer composition, e.g. different types of lipids and the percentage of cholesterol.

In literature there are several studies about the interaction between amyloid protein, i.e. monomer and small oligomer, and different type of bilayer. Studies reported here analyse the effects of amyloid protein on POPC bilayer. *Xiang et al.*[89] found that oligomers with more than two peptides tend to modify the lipid bilayer by generating water channels, besides, with the increasing of the number of peptides the free energy of penetration tends to decrease. In another work[97] authors conclude that in case of carpeting of amyloid peptide on the membrane, the latter undergo perturbation becoming more gel-like and rigid modifying area per lipid and order parameter. Nevertheless, since POPC is a zwitterionic bilayer, both the membrane and the protein inserted in it tend to remain stable during MD simulations[81,82]. Other MD studies demonstrate that the insertion of Aβ oligomers into explicit solvated lipid bilayer is not spontaneous due to high energy barrier[98]. However, once an oligomer is inserted into the membrane, it causes a thinning of the bilayer and this consequences increase with the assembly dimension[99]. Also, *Jang et al.*, simulating pore formation starting from small Aβ40 fibre, found that consequences of insertion into the bilayer are local thinning, membrane

disruption and local increasing of the surface pressure. Another consequence of Aβ association with cell membrane is cytotoxic effect due to an increase in membrane fluidity[100].

Starting from these observations, the aim of this chapter is to analyse the effects between Aβ$_{11-42}$ protein and 1-palmitoyl-2-oleoyl-sn-glycero-3-phosphocholine (POPC) bilayer. In particular, a peptide, an oligomer and a fibre are inserted into the lipid bilayer.

4.2   Material and Methods

4.2.1 Systems setup: protein in water

Initial simulations were performed to characterize Aβ$_{11-42}$ peptide, 5-mer oligomer and 5-mer fibre behaviour in water. Both the peptide and the fibre were extracted from Protein Data Bank (PDB ID: 1IYT[101] and 2MXU[102], respectively), while the oligomer was obtained from the monomer simulation.

Protein and fibre were inserted into a triclinic box placed respectively at a distance of 2 nm and 1.2 nm from the edge of the box to respect the minimum image condition. Boxes were solvated with explicit water and 0.15 M ions concentration was set, with counterions included to maintain a net neutral system. After the equilibration, 300 ns for each system were simulated.

Instead, to obtain the oligomer, a peptide representative structure was extracted from the last 100 ns and its five repetitions were placed randomly in a box. Each monomer was separated from the other and from the edge of the box at least by 1.2 nm to avoid long range interaction. Also in this case, the system was solvated with water, neutralized with counterions and 0.15 M NaCl was added. After 500 ns of MD simulation, an oligomer conformation was selected and inserted into the bilayer. This process was referred to the one used in another work[103].

4.2.2 Systems setup: protein in membrane

To evaluate the impact of amyloid β assemblies on the membrane, a peptide, a 5-mer oligomer and a 5-mer fibre were inserted into a POPC bilayer using CHARMM-GUI[104–106] software (Figure 14). A lipid bilayer of 14 nm x 14 nm was created and a layer of water of 2 nm was added over and under the membrane. Configurations were neutralized with counterions and the ions concentration was fixed at 0.15 M. Each system has between 140000 and 170000 particles.

Peptide and oligomer were inserted into the bilayer with casual orientation, while, in order to create different replicas, the fibre was oriented in a different way for every system (see Supporting Information).

Similarly, a POPC bilayer was created with the same dimensions as above, except for the 1 nm of water thickness. This membrane system was used to compare the results obtained from the above-mentioned membrane protein systems.
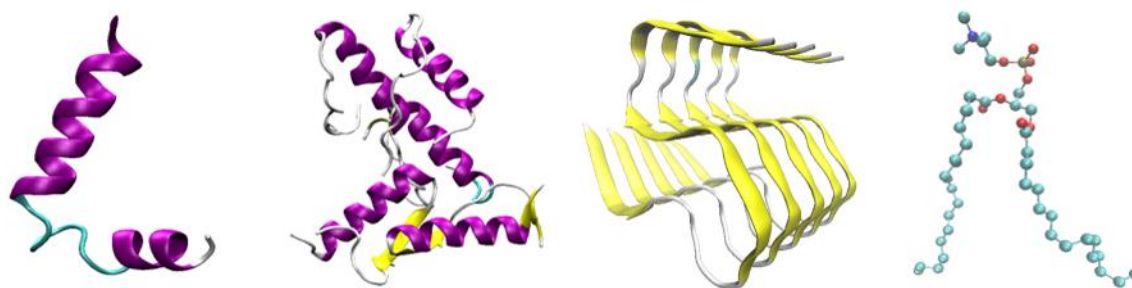
Figure 14 – Visualization of the systems' main component. Starting from the left are represented the peptide, the oligomer, the fibre and a POPC phospholipid

4.2.3 Simulation Setups

Simulations were performed using GROMACS software package, version 5.1.4[107]. The forcefield used was CHARMM36[108], and the system was solvated with explicit water, TIP3P model[109]. The systems were subjected to energy minimization, NVT ensemble, NPT ensemble and molecular dynamics (MD) production. Electrostatic was calculated using Particle Mesh Ewald (PME) algorithm[110] and Van der Waals with the cut-off of 1.2 nm.

The system was minimized by the steepest descent algorithm[7]. A NVT ensemble was simulated for 100 ps to reach a temperature of 300 K using V-rescale algorithm[111] and time constant of 0.1 ps. The correct density was achieved with 100 ps NPT equilibration using Berendsen algorithm[112] with a semi-isotropic coupling type. The MD production has been run for 300 ns for systems with only bilayer and only peptide, 100 ns for systems with protein and bilayer, and 500 ns for oligomer in solution. Nose-Hoover[113] and Parrinello-Rahman[112] were used as temperature and pressure coupling. Periodic boundary conditions were applied in all three dimensions.

Trajectories were extracted every 20 ps of simulation and the Visual Molecular Dynamics (VMD) package is used to display the simulated systems.

4.2.4 Protein Characterization

To analyse the membrane's effects on the protein, Root Mean Square Fluctuation (RMSF), Solvent Accessible Surface Area (SASA) and an order parameter were implemented.

To evaluate the structural stability of the fibre and the alignment among protein chains, an order parameter was developed. It was characterized by the following equation:

$$ordP = \frac{1}{N} \sum_{r=11}^{42} \frac{<v_r, x>}{||v_r|| \cdot ||x||} = \frac{1}{N} \sum_{r=11}^{42} cos\alpha$$

where v_r is the vector between C$_\alpha$-atom of each residue r of chain A and the corresponding C$_\alpha$-atom of the same residue of chain E (Figure 15) and x is the fibril axis. If $ordP$ is close to 1, the chains maintain an alignment to the initial structure; if the values are lower than 1, the overall structural order decrease. This order parameter has been used in a recent computational study on amyloid protein[49].
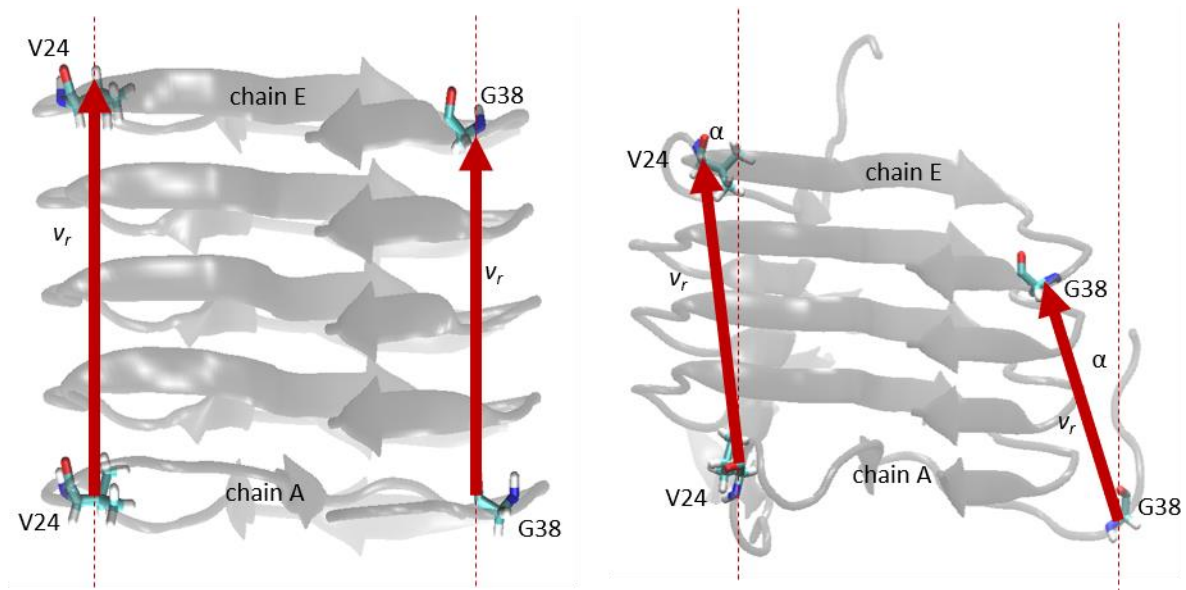

Figure 15 – The order parameter was implemented to analyse the alignment among fibre's chains. v_r is the vector between C$_\alpha$-atom of each residue r of chain A and the corresponding C$_\alpha$-atom of the same residue of chain E

4.2.5 Membrane Characterization

To analyse the conformational properties of the membrane, area per lipid (APL) and bilayer thickness were obtained using GridMAT-MD tool[114] with 100x100 grid points.

While, the order parameter (ρ_r) was implemented to study the orientation of POPC lipids. It was calculated using the following equation:

$$\rho_r = \left| \left\langle \frac{3cos^2\theta - 1}{2} \right\rangle \right|$$

where θ is the angle between the lipid identifier vector (see Supporting Information) and z-axis, normal to the membrane. The angle brackets indicate the time average over all atoms located inside a certain circular crown. Circular crowns were 1 nm thick and were determinate on function of the distance from the protein. The order parameter varies between 1, indicating full order along the interface normal, and -1/2, denoting full order along the perpendicular to the interface normal.

The membrane bending modulus (K_c) was calculated with the method explain in a *Khelashvili et al.* work[20], which suggest a heuristic approximation for calculating the monolayer bending modulus from MD trajectories. The bending modulus is correlated with the ability of the lipid membrane component to change orientation respect each other. This lipid ability is described by the splay angle (α, between 0° and 90°) which is related to the splay module χ_{12}. The potential mean force ($PMF(\alpha)$) was obtained from the probability distribution $P(\alpha)$ of the splay angle:

$$PMF(\alpha) = -k_B T ln\left[\frac{P(\alpha)}{P_0(\alpha)} \right]$$

where $P_0(\alpha) = sin(\alpha)$ is the probability distribution of a hypothetical non-interacting particle system[19], k_B is the factor of Boltzmann and T is the temperature of the system. Fitting the $PMF(\alpha)$ data with a quadratic function permits to obtain the tilt module χ and the splay module χ_{12}. Then:

$$\frac{1}{k_m} = \frac{1}{\phi_{total}} \sum_{\langle i,j \rangle} \frac{\phi_{ij}}{\chi_{12}^{ij}}$$

Where χ_{12}^{ij} is the splay modulus for the *ijth* pair type, ϕ_{ij} is the number of near-neighbouring *ij* encounter pairs, obtained directly from MD trajectories, and $\phi_{total} = \sum_{ij} \phi_{ij}$ represents the total number of encounters in the simulation for all possible pairwise contributions $\langle i,j \rangle$ for which the splay is calculated. Since the bilayer was composed by only POPC, the splay module corresponds to k_m.

Using the heuristic approximation, the bilayer bending module was:

$$K_C = 2k_m$$

Bending modulus has been calculated also in function of the distance from the protein, 2 nm thick circular crowns were isolated. The value obtained are reported in function of the mean radius.

4.3 Results

In this section, results from the analysis explained above are showed. The first part focuses on the protein characterization and the second part on the membrane characterization. All the results are computed on the last 20 ns, except for the oligomer in water, where analysis is made between 270 and 290 ns.

Figure 16 displays the final state of MD simulations of systems constituted by the protein and the membrane. The initial states are reported in supporting information.
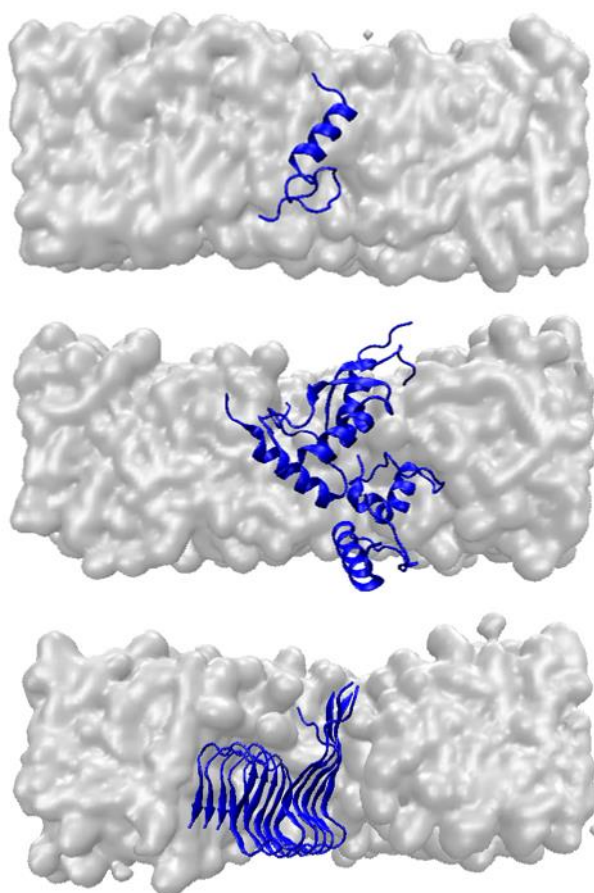
Figure 16 - Representation of the final states for each system studies. From the top: the peptide, the oligomer and the fibre.

4.3.1 Conformation of Aβ11-42 protein in water and in membrane

Protein fluctuations are evaluated with Root Mean Square Fluctuation (RMSF) analysis (Figure 17). In all cases, protein in water fluctuates more than the protein in membrane; this difference is marked for the peptide (Figure 17A) and the oligomer (Figure 17B). Since the fibre is more stable, principal differences are reported only on the C-terminal part, from residue V36, because of the exposure to the solvent (Figure 17C).
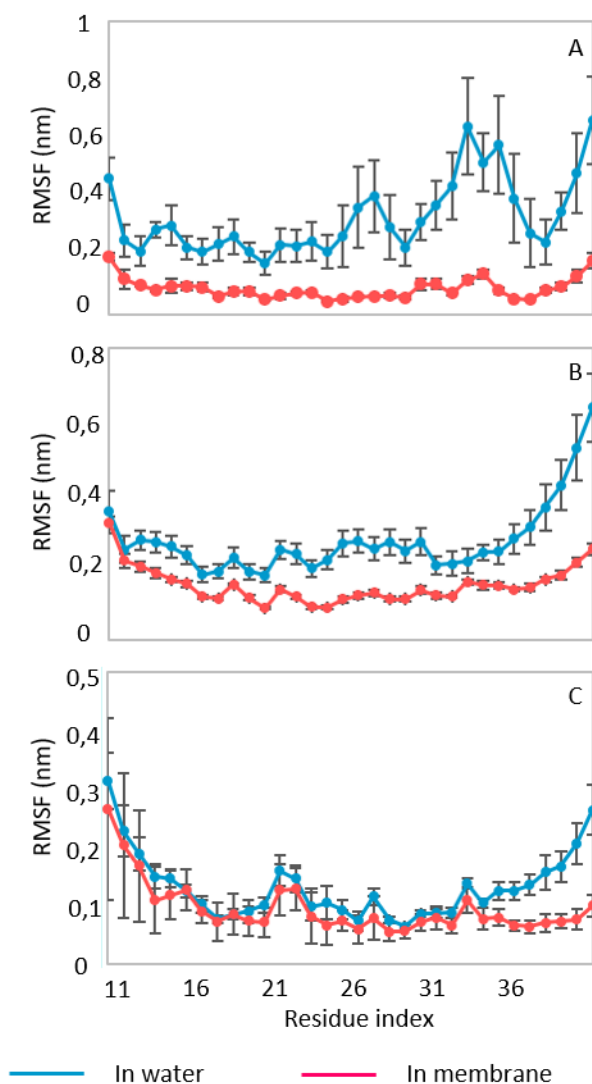
Figure 17 – Protein fluctuations are analysed using Root Mean Square Fluctuations (RMSF). A) shows RMSF for Aβ peptide both in water and in membrane, B) displays RMSF for the oligomer both in solution and inserted into POPC bilayer, C) contains the RMSF trend for the fibre both in water and in membrane.

Furthermore, the Solvent Accessible Surface Area (SASA) per residue is calculated to study the tendency of each residues of exposing itself to the solvent (Figure 18). Proteins tend to have the same behaviour in water and in membrane. Observing the graph referred to peptide (Figure 18A), some differences can be noted for residues F20, I32 and I41 where values are higher for the protein in membrane. In case of oligomer (Figure 18B), a difference can be noted between residues I31 and V36 where values are higher for the assembly in membrane. In Figure 18C fibre shows the same behaviour in water and in membrane.
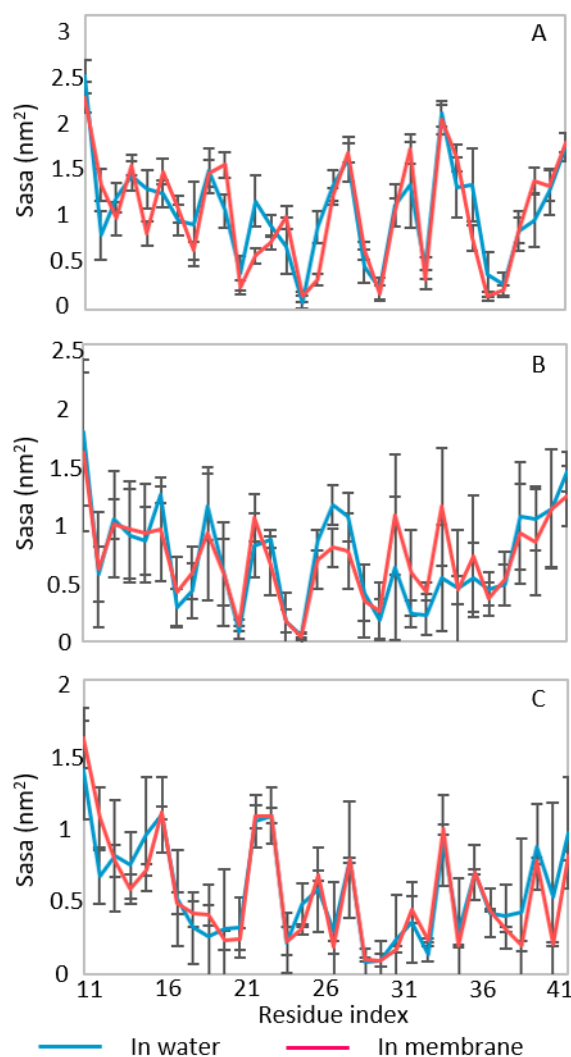
Figure 18 - Solvent Accesible Surface Area (SASA) is calculate. A) represents SASA trend for peptide both in water and in membrane, B) is for oligomer in water and in membrane and C) is for fibre both in water and in membrane.

Also, the calculation of total SASA shows that the peptide and the oligomer have similar behaviour both in water and in membrane. As regards the fibre, a small difference is observed; in fact, the SASA value for the fibre in water (91.0 ± 1.9) nm^2 is slightly higher than the fibre in lipid bilayer (87.8 ± 3.7) nm^2.

The mean value and standard deviation of inter-chain contact area are calculated and reported in Figure 19 for the oligomer and the fibre. This graph highlights the differences between the two assemblies. In fact, the fibre, that is more compact, is characterized by a high contact area and low standard deviation, while the oligomer tends to expose more the hydrophilic part as it is characterized by low mean value and high standard deviation. This mean that the fibre remains stable and compact in membrane unlike the oligomer that is disordered and more exposed to the solvent.
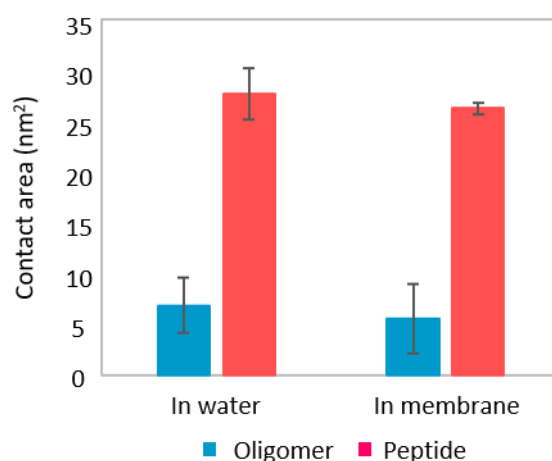
Figure 19 - Contact area. The fibre is characterized by a high contact area and low standard deviation, while the oligomer tends is characterized by low mean value and high standard deviation as it tends to expose the hydrophilic part.

Finally, the order parameter is valuated for the fibre. Since the fibre is characterized by a high stability, the order is maintained both when the protein is in solution (0.979 ± 0.004) and when it is inserted in membrane (0.971 ± 0.007).

4.3.2 Effects on POPC bilayer by Aβ$_{11-42}$ protein

Area per lipid is directly related with the bilayer fluidity. The value obtained for only membrane is (61.6 ± 0.2) Å^2 and it is considered as reference in calculation of percentage variation (Figure 20A). This value is comparable to the one obtained from both experimental and simulation works $(64.0 \pm 1.5$ Å$)$[97,115–117].

However, when the protein is in the membrane there is an increase in APL value. In particular, with peptide there is an increase of about 2.0%, with oligomer of 8.2% and with fibre of 8.6% (Figure 20A). Therefore, assemblies tend to destabilize the membrane more than the peptide.

Consequence of insertion of Aβ protein into lipid bilayer is, also, a decrease in bilayer thickness (Figure 20B); the only membrane is characterised by a thickness of (4.02 ± 0.02) nm. With peptide the value remains almost unchanged as only decrease by 0.9%, assemblies have major influence, as both oligomer and fibre reduce the value by 3.9%.
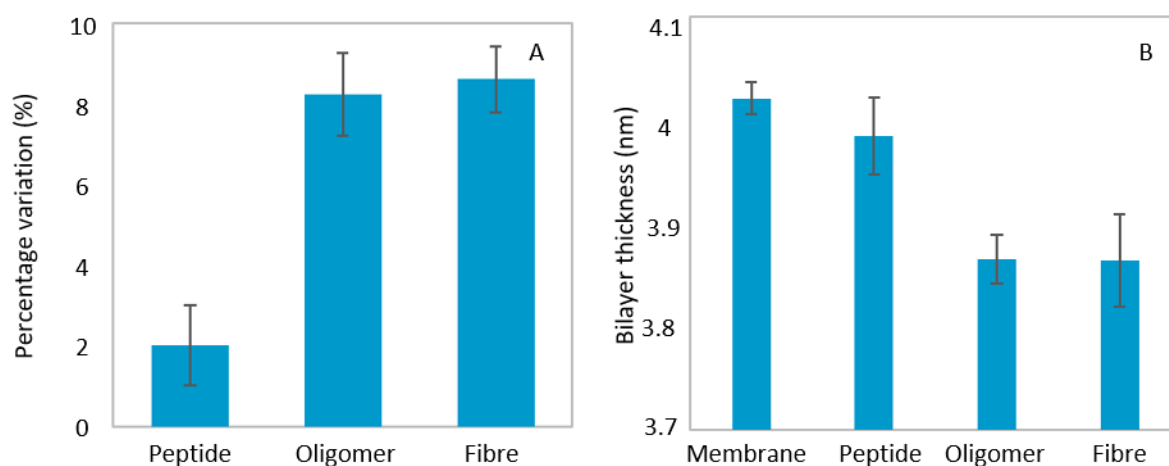

Figure 20 – A) represents the area per lipid percentage variation referred to the one obtained for the only membrane (61.6 ± 0.2) Å^2, while B) shows the bilayer thickness, the insertion of assemblies into the bilayer causes membrane thinning of 3.9%.

Order parameter is reported as function of the distance of the POPC lipid from the protein; in case of only membrane the distance is referred to the centre of the bilayer (Figure 21). To obtain order parameter in function of the distance, 1 nm thick circular crown are isolated, and the value is showed in correspondence of the mean radius.

Near the protein the bilayer is less ordered than the only membrane especially in case of oligomer and fibre. Order is restored increasing the distance from the assembly, over 4 nm from the proteins' centre of mass. With peptide, order parameter does not undergo major changes.
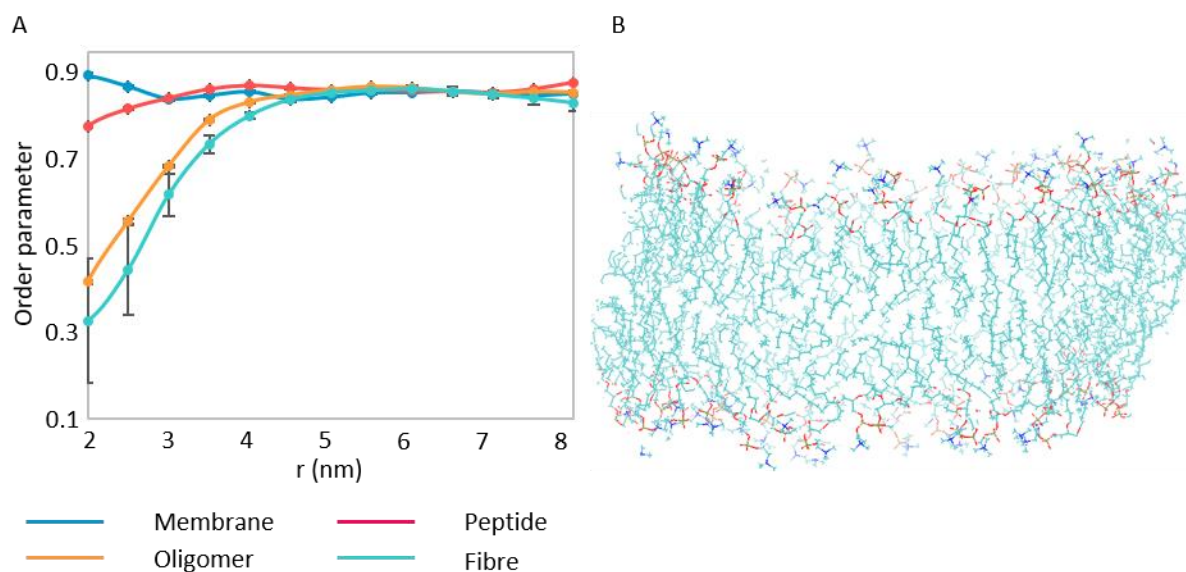
Figure 21 - A) represents of the order parameter in function of the distance from the centre of mass of the protein. In case of only membrane, the distance is referred to the centre of the bilayer. 1nm thick circular crown are isolated and the order parameter calculated is represented in correspondence of the mean radius. B) contains a visualization of a lipid band centred in 2 nm extracted from the system with the oligomer.

Finally, membrane mechanical properties are evaluated. An estimation of the bending module is showed in Figure 22. In particular, left panel shows percentage variation referred to the membrane. In case of only membrane, a bending modulus of (21.5 ± 0.4) k_BT is reached, while when the protein is inside the bilayer the bending module decrease. In case of peptide there is a decrease of 1.8%. Marked decrease is noted in case of oligomer and fibre, respectively of 18.0% and 14.6%.

In right panel is analyse the bending modulus in function of the distance from the protein. It is calculated considering 2nm thick circular crown and reporting the value in correspondence of the mean radius. Near assemblies there is a drastically decreased of the bending modulus, reaching 12.7 k_BT for the fibre and 13.2 k_BT for the oligomer. Moving away from the protein, the value obtained for the only membrane is not achieved, this means that assemblies have also long-range influences. Considering the peptide, there is a variation depending on the distance, but values oscillate around that of the only membrane.
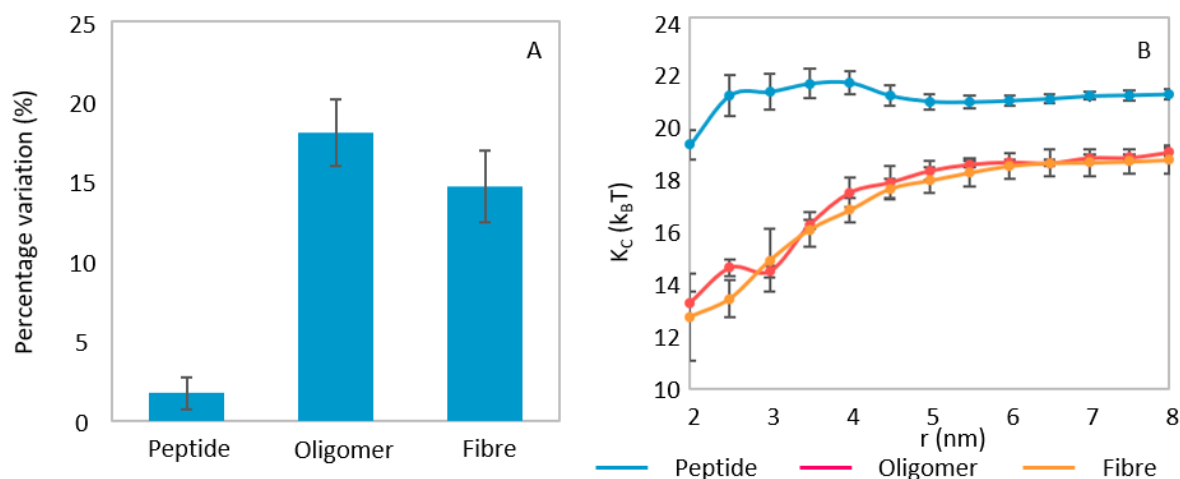
Figure 22 – Bending modulus percentage variation refered to the value for only membrane (21.5 ± 0.4) k_BT (A) and variation of mechanical properties in function of the distance fom the centre of mass of the protein (B) are here reported. Assemmblies tend to destabilize the bilayer more than the pepdite. In particular the major influences is found in first 4.5 nm from the aggregates centre of mass. Moving away from the protein, bilayer mechanical properties are not restored.

Observing the results, it can be seen that the protein is not affected by the interaction with the membrane, since no significant changes are observed on the analysis carried out. On the contrary, the membrane is destabilized by the presence of the protein. In particular, unlike the peptide that does not change much the lipid bilayer, oligomer and fibre modify in the same way the area per lipid and bilayer thickness but in different ways the tilt and splay angle. Moreover, variations in order parameter and bending modulus are related to the distance from the proteins' centre of mass.

4.4   Discussion

AD is a neurodegenerative disease characterized by the deposition of Aβ plaques. Aβ peptide has two principal isoforms: Aβ$_{40}$, that is 40-residues long, and Aβ$_{42}$, that is 42-residues long. Even if Aβ$_{42}$ is present in smaller quantity than Aβ$_{40}$, it is the principal component of the diffusive deposits[118]. The interaction of small fibres or oligomers within the neuronal membrane causes toxicity and progression of AD. In fact, Aβ is able to insert itself into the bilayer causing severe membrane damage. The influence between the protein and the membrane depends on the type of lipids that make up the membrane. In this work the bilayer consists of only zwitterionic POPC phospholipids, because they constitute eukaryotic cell membrane and PC lipids are abundant in neuronal membrane[119].

In all the cases, the protein tends to stay inside the bilayer. This is compatible with what found by *Xiao et al.*[102], where their results shows that trimer and pentamer remain inside the membrane, differently to monomer and dimer. Even if in this case peptide remains inside the membrane probably for the short duration of the simulation. The protein does not undergo changes if inserted into POPC bilayer. Other studies[79,80] report the same conclusion, this happen because lipids have zwitterionic characteristic and tend to not modify protein's properties.

On other hand, the membrane undergoes some modification, especially when the assemblies are embedded. Contrary to what happens in literature[97], there is an increase in area per lipid because some lipids tend to surround the protein moving toward the centre of the bilayer. However, an increase in APL is related with an increase in membrane fluidity, compatible with the decrease in bending modulus.

The decrease in bilayer thickness is comparable with results from other works[120,121].

More interesting are the variation in order parameter and bending modulus. In case of bending modulus, results obtained for only membrane are in agreement with literature 20.3 k_BT[122] and (24.6 ± 2.6) k_BT[123]. Variations in order parameter are observed also in other studies[81,97]. The trend of these properties shows that Aβ assemblies influence is enclosed in the first 4.5 nm from the proteins' centre of mass. Exceeded this radius the order parameter is recovered unlike the bending modulus that reaches a plateau at a lower value respect the one for only membrane, as if there were a long-range interaction of the protein. Since, there will not be a single assembly inserted into the membrane, this result can be useful to predict the effect on the bilayer depending on the number of embedded proteins or to provide how many aggregates are needed to destabilize the cell membrane.

4.5 Conclusions

In this chapter, effects of different conformation of Aβ$_{11\text{-}42}$ peptide inserted into POPC bilayer are analysed. Molecular Dynamics simulations of Aβ$_{11\text{-}42}$ peptide, oligomer and fibre embedded into membrane are performed to study the assemblies' impact on membrane conformational stability and dynamics. MD results shows that proteins remain almost unchanged as showed in other works[81,82]. Despite, the membrane highlights changes in order and mechanical properties. Unlike the peptide that does not change much the lipid bilayer, oligomer and fibre modify in the same way the area per lipid and bilayer thickness but in

different ways the tilt and splay angle. In particular, the bending modulus and the order parameter are influenced by the distance from the assemblies' centre of mass. Furthermore, moving away from the protein, the order parameter is re-established while the bending module reaches a constant value lower than the one of the only membrane.

Chapter 5

CONCLUSIONS AND FUTURE PERSPECTIVE

Despite Alzheimer's disease (AD) is the most common form of dementia, the onset mechanism is still unclear. Many hypotheses have been put forward, but the most accredited is the amyloid cascade hypothesis, which considers the amyloid plaque formation the principal cause in AD development. In fact, Amyloid β (Aβ) peptide deposits tend to aggregate forming both ordered and disordered structures. Amyloid assemblies, during their formation, interact with neuronal membrane causing cell death and memory loss through different pathways. A better understanding of the effects of these interactions can be useful in research, since no treatments are able to slow down or cure the disorder. Molecular Dynamics (MD) simulations allow to provide quantitative and dynamics information of cell membrane behaviour.

In this Master Thesis work MD simulations are employed to analyse the impact of Aβ$_{11-42}$ assemblies on membrane conformational stability and dynamics. For this purpose, Aβ peptide and both ordered and disordered pentamer are inserted into POPC bilayer. Since POPC has zwitterionic characteristics, proteins do not change their properties. On the contrary, the membrane undergoes some changes, especially when oligomer and fibre are embedded into the bilayer. An increase in bilayer fluidity is highlighted first by the area per lipid and then by the decrease in bending module. Another result that validates the increase in lipids fluidity is the variation of the lipids' order parameter around the protein. All these changes are observed in a neighbourhood of 4.5 nm from the centre of mass of the aggregates and these results can be useful to predict the number of aggregates needed to destabilize the cell membrane.

This study was focused on the investigation of POPC membrane stability and dynamics after the insertion of Aβ pentamer. Further work could be done to provide a more in-depth view using different membrane models enriched by several lipid types, e.g., cholesterol. In addition, the use of different size oligomer would lead to a better understanding of the impact of Aβ aggregates on cell membrane.

ACKNOWLEDGEMENT

REFERENCES

(1)   Gaugler, J.; James, B.; Johnson, T.; Scholz, K.; Weuve, J. 2016 Alzheimer's Disease Facts and Figures. *Alzheimer's Dement.* **2016**, *12* (4), 459–509. https://doi.org/10.1016/j.jalz.2016.03.001.

(2)   Crabbe, J. Molecular Modelling: Principles and Applications. *Comput. Chem.* **1997**, *21* (3), 185. https://doi.org/10.1016/S0097-8485(96)00029-0.

(3)   Johnson, J. K.; Zollweg, J. A.; Gubbins, K. E. The Lennard-Jones Equation of State Revisited. *Mol. Phys.* **1993**, *78* (3), 591–618. https://doi.org/10.1080/00268979300100411.

(4)   Deserno, M.; Holm, C. How to Mesh up Ewald Sums. I. a Theoretical and Numerical Comparison of Various Particle Mesh Routines. *Journal of Chemical Physics*. July 7, 1998, pp 7678–7693. https://doi.org/10.1063/1.477414.

(5)   Lin, Y.; Baumketner, A.; Deng, S.; Xu, Z.; Jacobs, D.; Cai, W. An Image-Based Reaction Field Method for Electrostatic Interactions in Molecular Dynamics Simulations of Aqueous Solutions. *J. Chem. Phys.* **2009**, *131* (15), 154103. https://doi.org/10.1063/1.3245232.

(6)   Ding, H. Q.; Karasawa, N.; Goddard, W. A. The Reduced Cell Multipole Method for Coulomb Interactions in Periodic Systems with Million-Atom Unit Cells. *Chem. Phys. Lett.* **1992**, *196* (1–2), 6–10. https://doi.org/10.1016/0009-2614(92)85920-6.

(7)   Fletcher, R.; Powell, M. J. D. A Rapidly Convergent Descent Method for Minimization. *Comput. J.* **1963**, *6* (2), 163–168. https://doi.org/10.1093/comjnl/6.2.163.

(8)   Powell, M. J. D.; J., M. Restart Procedures for the Conjugate Gradient Method. *Math. Program.* **1977**, *12* (1), 241–254. https://doi.org/10.1007/BF01593790.

(9)   Helfrich, W. Elastic Properties of Lipid Bilayers: Theory and Possible Experiments. *Z. Naturforsch. C. 28* (11), 693–703.

(10)   Lundbaek, J. CAPSAICIN REGULATES VOLTAGE-DEPENDENT SODIUM CHANNELSBY ALTERING LIPID BILAYER ELASTICITY. *Mol. Pharmacol.* **2005**, *68* (3), 680–689. https://doi.org/10.1124/mol.105.013573.

(11) Döbereiner, H. G.; Gompper, G.; Haluska, C. K.; Kroll, D. M.; Petrov, P. G.; Riske, K. A. Advanced Flicker Spectroscopy of Fluid Membranes. *Phys. Rev. Lett.* **2003**, *91* (4), 048301. https://doi.org/10.1103/PhysRevLett.91.048301.

(12) Lindahl, E.; Edholm, O. Mesoscopic Undulations and Thickness Fluctuations in Lipid Bilayers from Molecular Dynamics Simulations. *Biophys. J.* **2000**, *79* (1), 426–433. https://doi.org/10.1016/S0006-3495(00)76304-1.

(13) Nagle, J. F.; Edholm, O.; Braun, A. R.; Brandt, E. G.; Sachs, J. N. Interpretation of Fluctuation Spectra in Lipid Bilayer Simulations. *Biophys. J.* **2011**, *100* (9), 2104–2111. https://doi.org/10.1016/j.bpj.2011.03.010.

(14) Hofsäß, C.; Lindahl, E.; Edholm, O. Molecular Dynamics Simulations of Phospholipid Bilayers with Cholesterol. *Biophys. J.* **2003**, *84* (4), 2192–2206. https://doi.org/10.1016/S0006-3495(03)75025-5.

(15) Watson, M. C.; Brandt, E. G.; Welch, P. M.; Brown, F. L. H. Determining Biomembrane Bending Rigidities from Simulations of Modest Size. *Phys. Rev. Lett.* **2012**, *109* (2), 028102. https://doi.org/10.1103/PhysRevLett.109.028102.

(16) Landau, L. D. (Lev D.; Lifshит͡s, E. M. (Evgeniĭ M.; Kosevich, A. M.; Pitaevskiĭ, L. P. (Lev P. *Theory of Elasticity*; Butterworth-Heinemann, 1986.

(17) Rawicz, W.; Olbrich, K. C.; McIntosh, T.; Needham, D.; Evans, E. A. Effect of Chain Length and Unsaturation on Elasticity of Lipid Bilayers. *Biophys. J.* **2000**, *79* (1), 328–339. https://doi.org/10.1016/S0006-3495(00)76295-3.

(18) Picas, L.; Rico, F.; Scheuring, S. Direct Measurement of the Mechanical Properties of Lipid Phases in Supported Bilayers. *Biophys. J.* **2012**, *102* (1), L01-3. https://doi.org/10.1016/j.bpj.2011.11.4001.

(19) Khelashvili, G.; Pabst, G.; Harries, D. Cholesterol Orientation and Tilt Modulus in DMPC Bilayers. *J. Phys. Chem. B* **2010**, *114* (22), 7524–7534. https://doi.org/10.1021/jp101889k.

(20) Khelashvili, G.; Kollmitzer, B.; Heftberger, P.; Pabst, G.; Harries, D. Calculating the Bending Modulus for Multicomponent Lipid Membranes in Different Thermodynamic Phases. *J. Chem. Theory Comput.* **2013**, *9* (9), 3866–3871. https://doi.org/10.1021/ct400492e.

(21) Khelashvili, G.; Johner, N.; Zhao, G.; Harries, D.; Scott, H. L. Molecular Origins of Bending Rigidity in Lipids with Isolated and Conjugated Double Bonds: The Effect of Cholesterol. *Chem. Phys. Lipids* **2014**, *178*, 18–26. https://doi.org/10.1016/j.chemphyslip.2013.12.012.

(22) Nussbaum, R. L.; Ellis, C. E. Alzheimer's Disease and Parkinson's Disease. *N. Engl. J. Med.* **2003**, *348* (14), 1356–1364. https://doi.org/10.1056/nejm2003ra020003.

(23) Hurd, M. D.; Martorell, P.; Delavande, A.; Mullen, K. J.; Langa, K. M. Monetary Costs of Dementia in the United States. *N. Engl. J. Med.* **2013**, *368* (14), 1326–1334. https://doi.org/10.1056/NEJMsa1204629.

(24) Association, A. 2018 Alzheimer's Disease Facts and Figures. *Alzheimer's Dement.* **2018**, *12* (4), 459–509. https://doi.org/10.1016/j.jalz.2016.03.001.

(25) Hebert, L. E.; Beckett, L. A.; Scherr, P. A.; Evans, D. A. Annual Incidence of Alzheimer Disease in the United States Projected to the Years 2000 through 2050. *Alzheimer Dis. Assoc. Disord. 15* (4), 169–173.

(26) Wimo, A.; Graff, C.; Knapp, M.; Fratiglioni, L.; Nordberg, A.; Brodaty, H.; Kivipelto, M.; Cedazo-Minguez, A.; Frisoni, G. B.; Georges, J.; et al. Defeating Alzheimer's Disease and Other Dementias: A Priority for European Science and Society. *Lancet Neurol.* **2016**, *15* (5), 455–532. https://doi.org/10.1016/s1474-4422(16)00062-4.

(27) Rizzuto, D.; Bellocco, R.; Kivipelto, M.; Clerici, F.; Wimo, A.; Fratiglioni, L. Dementia after Age 75: Survival in Different Severity Stages and Years of Life Lost. *Curr. Alzheimer Res.* **2012**, *9* (7), 795–800.

(28) Sando, S. B.; Melquist, S.; Cannon, A.; Hutton, M.; Sletvold, O.; Saltvedt, I.; White, L. R.; Lydersen, S.; Aasly, J. Risk-Reducing Effect of Education in Alzheimer's Disease. *Int. J. Geriatr. Psychiatry* **2008**, *23* (11), 1156–1162. https://doi.org/10.1002/gps.2043.

(29) Fitzpatrick, A. L.; Kuller, L. H.; Ives, D. G.; Lopez, O. L.; Jagust, W.; Breitner, J. C. S.; Jones, B.; Lyketsos, C.; Dulberg, C. Incidence and Prevalence of Dementia in the Cardiovascular Health Study. *J. Am. Geriatr. Soc.* **2004**, *52* (2), 195–204.

(30) Jin, Y.-P.; Gatz, M.; Johansson, B.; Pedersen, N. L. Sensitivity and Specificity of Dementia Coding in Two Swedish Disease Registries. *Neurology* **2004**, *63* (4), 739–741.

(31) Brunnström, H. R.; Englund, E. M. Cause of Death in Patients with Dementia Disorders. *Eur. J. Neurol.* **2009**, *16* (4), 488–492. https://doi.org/10.1111/j.1468-1331.2008.02503.x.

(32) Burns, A.; Jacoby, R.; Luthert, P.; Levy, R. Cause of Death in Alzheimer's Disease. *Age Ageing* **1990**, *19* (5), 341–344.

(33) Hao, W.; Friedman, A. Mathematical Model on Alzheimer's Disease. *BMC Syst. Biol.* **2016**, *10* (1), 108. https://doi.org/10.1186/s12918-016-0348-2.

(34) Ossenkoppele, R.; Raijmakers, P. G. H. M.; Scheltens, P.; van Berckel, B. N. M.; Scherder, E. J. A.; Groot, C.; Hooghiemstra, A. M.; van der Flier, W. M. The Effect of Physical Activity on Cognitive Function in Patients with Dementia: A Meta-Analysis of Randomized Control Trials. *Ageing Res. Rev.* **2015**, *25*, 13–23. https://doi.org/10.1016/j.arr.2015.11.005.

(35) Alzheimer, A. Über Eigenartige Krankheitsfälle Des Späteren Alters. *Gesamte Neurol Psychiatr.* **1911**, *4* (356), 385. https://doi.org/10.1007/BF02866241.

(36) Davies, P.; Maloney, A. J. Selective Loss of Central Cholinergic Neurons in Alzheimer's Disease. *Lancet (London, England)* **1976**, *2* (8000), 1403.

(37) Terry, R. D. The Pathogenesis of Alzheimer Disease: An Alternative to the Amyloid Hypothesis. *J. Neuropathol. Exp. Neurol.* **1996**, *55* (10), 1023–1025. https://doi.org/10.1097/00005072-199655100-00001.

(38) Hardy, J. A.; Higgins, G. A. Alzheimer's Disease: The Amyloid Cascade Hypothesis. *Science* **1992**, *256* (5054), 184–185.

(39) De la Torre, J. C.; Mussivand, T. Can Disturbed Brain Microcirculation Cause Alzheimer's Disease? *Neurological Research*. Taylor & Francis June 20, 1993, pp 146–153. https://doi.org/10.1080/01616412.1993.11740127.

(40) Barage, S. H.; Sonawane, K. D. Amyloid Cascade Hypothesis: Pathogenesis and Therapeutic Strategies in Alzheimer's Disease. *Neuropeptides*. August 2015, pp 1–18. https://doi.org/10.1016/j.npep.2015.06.008.

(41) Roy, S.; Zhang, B.; Lee, V. M.-Y.; Trojanowski, J. Q. Axonal Transport Defects: A Common Theme in Neurodegenerative Diseases. *Acta Neuropathologica*. January 12, 2005, pp 5–13. https://doi.org/10.1007/s00401-004-0952-x.

(42) Guo, Q.; Fu, W.; Sopher, B. L.; Miller, M. W.; Ware, C. B.; Martin, G. M.; Mattson, M. P. Increased Vulnerability of Hippocampal Neurons to Excitotoxic Necrosis in Presenilin-1 Mutant Knock-in Mice. *Nat. Med.* **1999**, *5* (1), 101–106. https://doi.org/10.1038/4789.

(43) Haass, C.; Selkoe, D. J. Soluble Protein Oligomers in Neurodegeneration: Lessons from the Alzheimer's Amyloid β-Peptide. *Nature Reviews Molecular Cell Biology*. February 1, 2007, pp 101–112. https://doi.org/10.1038/nrm2101.

(44) de la Torre, J. The Vascular Hypothesis of Alzheimer's Disease: A Key to Preclinical Prediction of Dementia Using Neuroimaging. *J. Alzheimers. Dis.* **2018**, *63* (1), 35–52. https://doi.org/10.3233/JAD-180004.

(45) Glenner, G. G.; Wong, C. W. Alzheimer's Disease: Initial Report of the Purification and Characterization of a Novel Cerebrovascular Amyloid Protein. *Biochem. Biophys. Res. Commun.* **1984**, *120* (3), 885–890. https://doi.org/10.1016/S0006-291X(84)80190-4.

(46) Li, M.; Chen, L.; Lee, D. H. S.; Yu, L. C.; Zhang, Y. The Role of Intracellular Amyloid β in Alzheimer's Disease. *Progress in Neurobiology*. July 2007, pp 131–139. https://doi.org/10.1016/j.pneurobio.2007.08.002.

(47) Lee, H. J.; Korshavn, K. J.; Nam, Y.; Kang, J.; Paul, T. J.; Kerr, R. A.; Youn, I. S.; Ozbil, M.; Kim, K. S.; Ruotolo, B. T.; et al. Structural and Mechanistic Insights into Development of Chemical Tools to Control Individual and Inter-Related Pathological Features in Alzheimer's Disease. *Chem. - A Eur. J.* **2017**, *23* (11), 2706–2715. https://doi.org/10.1002/chem.201605401.

(48) Xi, W.; Wang, W.; Abbott, G.; Hansmann, U. H. E. Stability of a Recently Found Triple-β-Stranded Aβ1–42 Fibril Motif. *J. Phys. Chem. B* **2016**, *120* (20), 4548–4557. https://doi.org/10.1021/acs.jpcb.6b01724.

(49) Grasso, G.; Rebella, M.; Muscat, S.; Morbiducci, U.; Tuszynski, J.; Danani, A.; Deriu, M. A. Conformational Dynamics and Stability of U-Shaped and s-Shaped Amyloid β Assemblies. *Int. J. Mol. Sci.* **2018**, *19* (2), 571. https://doi.org/10.3390/ijms19020571.

(50) Wu, J. W.; Glabe, C. G.; Lednev, I. K.; Breydo, L.; Rasool, S.; Uversky, V. N.; Kurouski, D.; Milton, S. Structural Differences between Amyloid Beta Oligomers.

Biochem. Biophys. Res. Commun. **2016**, *477* (4), 700–705. https://doi.org/10.1016/j.bbrc.2016.06.122.

(51)   Sengupta, U.; Nilson, A. N.; Kayed, R. The Role of Amyloid-β Oligomers in Toxicity, Propagation, and Immunotherapy. *EBioMedicine*. Elsevier April 2016, pp 42–49. https://doi.org/10.1016/j.ebiom.2016.03.035.

(52)   Arora, A.; Ha, C.; Park, C. B. Insulin Amyloid Fibrillation at above 100°C: New Insights into Protein Folding under Extreme Temperatures. *Protein Sci.* **2004**, *13* (9), 2429–2436. https://doi.org/10.1110/ps.04823504.

(53)   Tartaglia, G. G.; Cavalli, A.; Pellarin, R.; Caflisch, A. Prediction of Aggregation Rate and Aggregation-Prone Segments in Polypeptide Sequences. *Protein Sci.* **2005**, *14* (10), 2723–2734. https://doi.org/10.1110/ps.051471205.

(54)   Qiang, W.; Yau, W. M.; Schulte, J. Fibrillation of β Amyloid Peptides in the Presence of Phospholipid Bilayers and the Consequent Membrane Disruption. *Biochim. Biophys. Acta - Biomembr.* **2015**, *1848* (1), 266–276. https://doi.org/10.1016/j.bbamem.2014.04.011.

(55)   Pearson, H. A.; Peers, C. Physiological Roles for Amyloid β Peptides. *Journal of Physiology*. August 15, 2006, pp 5–10. https://doi.org/10.1113/jphysiol.2006.111203.

(56)   Fonseca, M. B.; Solá, S.; Xavier, J. M.; Dionísio, P. A.; Rodrigues, C. M. P. Amyloid β Peptides Promote Autophagy-Dependent Differentiation of Mouse Neural Stem Cells: Aβ-Mediated Neural Differentiation. *Molecular Neurobiology*. Springer US December 2, 2013, pp 829–840. https://doi.org/10.1007/s12035-013-8471-1.

(57)   Shankar, G. M.; Walsh, D. M. Alzheimer's Disease: Synaptic Dysfunction and Aβ. *Mol. Neurodegener.* **2009**, *4* (1), 48. https://doi.org/10.1186/1750-1326-4-48.

(58)   Parihar, M. S.; Brewer, G. J. Amyloid-β as a Modulator of Synaptic Plasticity. *Journal of Alzheimer's Disease*. IOS Press November 25, 2010, pp 741–763. https://doi.org/10.3233/JAD-2010-101020.

(59)   Garcia-Osta, A.; Alberini, C. M. Amyloid Beta Mediates Memory Formation. *Learn. Mem.* **2009**, *16* (4), 267–272. https://doi.org/10.1101/lm.1310209.

(60)   Zou, K.; Gong, J.-S.; Yanagisawa, K.; Michikawa, M. A Novel Function of Monomeric Amyloid β-Protein Serving as an Antioxidant Molecule against Metal-

Induced Oxidative Damage. *J. Neurosci.* **2002**, *22* (12), 4833–4841. https://doi.org/10.1523/jneurosci.22-12-04833.2002.

(61) Unnikrishnan, M. K.; Rao, M. N. A. Antiinflammatory Activity of Methionine, Methionine Sulfoxide and Methionine Sulfone. *Agents and Actions*. Birkhäuser-Verlag August 1990, pp 110–112. https://doi.org/10.1007/BF02003229.

(62) Sinha, M.; Bhowmick, P.; Banerjee, A.; Chakrabarti, S. Antioxidant Role of Amyloid β Protein in Cell-Free and Biological Systems: Implication for the Pathogenesis of Alzheimerdisease. *Free Radic. Biol. Med.* **2013**, *56*, 184–192. https://doi.org/10.1016/j.freeradbiomed.2012.09.036.

(63) Bond, P. J.; Khalid, S. Antimicrobial and Cell-Penetrating Peptides: Structure, Assembly and Mechanisms of Membrane Lysis via Atomistic and Coarse-Grained Molecular Dynamics Simulations. *Protein Pept. Lett.* **2010**, *17* (11), 1313–1327.

(64) Press-Sandler, O.; Miller, Y. Molecular Mechanisms of Membrane-Associated Amyloid Aggregation: Computational Perspective and Challenges. *Biochimica et Biophysica Acta - Biomembranes*. September 17, 2018, pp 1889–1905. https://doi.org/10.1016/j.bbamem.2018.03.014.

(65) Mayer, M.; Capone, R.; Sauer, A. M.; Bautista, M. R.; Yang, J.; Turner, R. S.; Prangkio, P.; Saluja, I.; Quiroz, F. G. Amyloid-β-Induced Ion Flux in Artificial Lipid Bilayers and Neuronal Cells: Resolving a Controversy. *Neurotox. Res.* **2009**, *16* (1), 1–13. https://doi.org/10.1007/s12640-009-9033-1.

(66) Quist, A.; Lin, H.; Frangione, B.; Lal, R.; Ghiso, J.; Ng, D.; Azimova, R.; Kagan, B.; Doudevski, I. Amyloid Ion Channels: A Common Structural Link for Protein-Misfolding Disease. *Proc. Natl. Acad. Sci.* **2005**, *102* (30), 10427–10432. https://doi.org/10.1073/pnas.0502066102.

(67) Brender, J. R.; Dürr, U. H. N.; Heyl, D.; Budarapu, M. B.; Ramamoorthy, A. Membrane Fragmentation by an Amyloidogenic Fragment of Human Islet Amyloid Polypeptide Detected by Solid-State NMR Spectroscopy of Membrane Nanotubes. *Biochim. Biophys. Acta - Biomembr.* **2007**, *1768* (9), 2026–2029. https://doi.org/10.1016/j.bbamem.2007.07.001.

(68) Engel, M. F. M.; Hoppener, J. W. M.; Meeldijk, H. J. D.; de Kruijff, B.;

Khemtemourian, L.; Kleijer, C. C.; Killian, J. A.; Jacobs, J.; Verkleij, A. J. Membrane Damage by Human Islet Amyloid Polypeptide through Fibril Growth at the Membrane. *Proc. Natl. Acad. Sci.* **2008**, *105* (16), 6033–6038. https://doi.org/10.1073/pnas.0708354105.

(69)   Hebda, J. A.; Miranker, A. D. The Interplay of Catalysis and Toxicity by Amyloid Intermediates on Lipid Bilayers: Insights from Type II Diabetes. *Annu. Rev. Biophys.* **2009**, *38* (1), 125–152. https://doi.org/10.1146/annurev.biophys.050708.133622.

(70)   Arispe, N.; Pollard, H. B.; Rojas, E. Giant Multilevel Cation Channels Formed by Alzheimer Disease Amyloid Beta-Protein [A Beta P-(1-40)] in Bilayer Membranes. *Proc. Natl. Acad. Sci. U. S. A.* **1993**, *90* (22), 10573–10577.

(71)   Shafrir, Y.; Durell, S.; Arispe, N.; Guy, H. R. Models of Membrane-Bound Alzheimer's Abeta Peptide Assemblies. *Proteins Struct. Funct. Bioinforma.* **2010**, *78* (16), 3473–3487. https://doi.org/10.1002/prot.22853.

(72)   Strodel, B.; Lee, J. W. L.; Whittleston, C. S.; Wales, D. J. Transmembrane Structures for Alzheimer's Aβ1-42oligomers. *J. Am. Chem. Soc.* **2010**, *132* (38), 13300–13312. https://doi.org/10.1021/ja103725c.

(73)   Shai, Y. Mechanism of the Binding, Insertion and Destabilization of Phospholipid Bilayer Membranes by α-Helical Antimicrobial and Cell Non-Selective Membrane-Lytic Peptides. *Biochimica et Biophysica Acta - Biomembranes*. December 15, 1999, pp 55–70. https://doi.org/10.1016/S0005-2736(99)00200-X.

(74)   Hellstrand, E.; Sparr, E.; Linse, S. Retardation of Aβ Fibril Formation by Phospholipid Vesicles Depends on Membrane Phase Behavior. *Biophys. J.* **2010**, *98* (10), 2206–2214. https://doi.org/10.1016/j.bpj.2010.01.063.

(75)   McLaurin, J.; Chakrabartty, A. Characterization of the Interactions of Alzheimer Beta-Amyloid Peptides with Phospholipid Membranes. *Eur. J. Biochem.* **1997**, *245* (2), 355–363.

(76)   Kremer, J. J.; Murphy, R. M. Kinetics of Adsorption of β-Amyloid Peptide Aβ(1-40) to Lipid Bilayers. *J. Biochem. Biophys. Methods* **2003**, *57* (2), 159–169. https://doi.org/10.1016/S0165-022X(03)00103-9.

(77)   Lin, M. S.; Chiu, H. M.; Fan, F. J.; Tsai, H. T.; Wang, S. S. S.; Chang, Y.; Chen, W. Y.

Kinetics and Enthalpy Measurements of Interaction between β-Amyloid and Liposomes by Surface Plasmon Resonance and Isothermal Titration Microcalorimetry. *Colloids Surfaces B Biointerfaces* **2007**, *58* (2), 231–236. https://doi.org/10.1016/j.colsurfb.2007.03.014.

(78) Williams, T. L.; Day, I. J.; Serpell, L. C. The Effect of Alzheimer's Aβ Aggregation State on the Permeation of Biomimetic Lipid Vesicles. *Langmuir* **2010**, *26* (22), 17260–17268. https://doi.org/10.1021/la101581g.

(79) Yu, X.; Wang, Q.; Pan, Q.; Zhou, F.; Zheng, J. Molecular Interactions of Alzheimer Amyloid-β Oligomers with Neutral and Negatively Charged Lipid Bilayers. *Phys. Chem. Chem. Phys.* **2013**, *15* (23), 8878–8889. https://doi.org/10.1039/c3cp44448a.

(80) Davis, C. H.; Berkowitz, M. L. A Molecular Dynamics Study of the Early Stages of Amyloid-β(1-42) Oligomerization: The Role of Lipid Membranes. *Proteins Struct. Funct. Bioinforma.* **2010**, *78* (11), 2533–2545. https://doi.org/10.1002/prot.22763.

(81) Ngo, S. T.; Hung, H. M.; Tran, K. N.; Nguyen, M. T. Replica Exchange Molecular Dynamics Study of the Amyloid Beta (11-40) Trimer Penetrating a Membrane. *RSC Adv.* **2017**, *7* (12), 7346–7357. https://doi.org/10.1039/c6ra26461a.

(82) Poojari, C.; Kukol, A.; Strodel, B. How the Amyloid-β Peptide and Membranes Affect Each Other: An Extensive Simulation Study. *Biochim. Biophys. Acta - Biomembr.* **2013**, *1828* (2), 327–339. https://doi.org/10.1016/j.bbamem.2012.09.001.

(83) Mason, R. P.; Shoemaker, W. J.; Shajenko, L.; Chambers, T. E.; Herbette, L. G. Evidence for Changes in the Alzheimer's Disease Brain Cortical Membrane Structure Mediated by Cholesterol. *Neurobiol. Aging* **1992**, *13* (3), 413–419. https://doi.org/10.1016/0197-4580(92)90116-F.

(84) MASON, R. P.; SHAJENKO, L.; HERBETTE, L. G. X-Ray Diffraction Analysis of Brain Lipid Membrane Structure in Alzheimer's Disease and B-Amyloid Peptide Interactions. *Ann. N. Y. Acad. Sci.* **1993**, *695* (1), 54–58. https://doi.org/10.1111/j.1749-6632.1993.tb23027.x.

(85) Ledesma, M. D.; Dotti, C. G. Amyloid Excess in Alzheimer's Disease: What Is Cholesterol to Be Blamed For? *FEBS Letters*. No longer published by Elsevier October 9, 2006, pp 5525–5532. https://doi.org/10.1016/j.febslet.2006.06.038.

(86)   Subasinghe, S.; Unabia, S.; Barrow, C. J.; Mok, S. S.; Aguilar, M. I.; Small, D. H. Cholesterol Is Necessary Both for the Toxic Effect of Aβ Peptides on Vascular Smooth Muscle Cells and for Aβ Binding to Vascular Smooth Muscle Cell Membranes. *J. Neurochem.* **2003**, *84* (3), 471–479. https://doi.org/10.1046/j.1471-4159.2003.01552.x.

(87)   Ashley, R. H.; Harroun, T. A.; Hauss, T.; Breen, K. C.; Bradshaw, J. P. Autoinsertion of Soluble Oligomers of Alzheimer's Aβ(1-42) Peptide into Cholesterol-Containing Membranes Is Accompanied by Relocation of the Sterol towards the Bilayer Surface. *BMC Struct. Biol.* **2006**, *6* (1), 21. https://doi.org/10.1186/1472-6807-6-21.

(88)   Yip, C. M.; Elton, E. A.; Darabie, A. A.; Morrison, M. R.; Mclaurin, J. Cholesterol, a Modulator of Membrane-Associated Aβ-Fibrillogenesis and Neurotoxicity. *J. Mol. Biol.* **2001**, *311* (4), 723–734. https://doi.org/10.1006/jmbi.2001.4881.

(89)   Xiang, N.; Lyu, Y.; Zhu, X.; Narsimhan, G. Investigation of the Interaction of Amyloid β Peptide (11-42) Oligomers with a 1-Palmitoyl-2-Oleoyl-Sn-Glycero-3-Phosphocholine (POPC) Membrane Using Molecular Dynamics Simulation. *Phys. Chem. Chem. Phys.* **2018**, *20* (10), 6817–6829. https://doi.org/10.1039/c7cp07148e.

(90)   Di Scala, C.; Yahi, N.; Boutemeur, S.; Flores, A.; Rodriguez, L.; Chahinian, H.; Fantini, J. Common Molecular Mechanism of Amyloid Pore Formation by Alzheimer's β-Amyloid Peptide and α-Synuclein. *Sci. Rep.* **2016**, *6* (1), 28781. https://doi.org/10.1038/srep28781.

(91)   Meleleo, D.; Galliani, A.; Notarachille, G. AβP1-42 Incorporation and Channel Formation in Planar Lipid Membranes: The Role of Cholesterol and Its Oxidation Products. *J. Bioenerg. Biomembr.* **2013**, *45* (4), 369–381. https://doi.org/10.1007/s10863-013-9513-0.

(92)   Bode, D. C.; Baker, M. D.; Viles, J. H. Ion Channel Formation by Amyloid-β 42 Oligomers but Not Amyloid-β 40 in Cellular Membranes. *J. Biol. Chem.* **2017**, *292* (4), 1404–1413. https://doi.org/10.1074/jbc.M116.762526.

(93)   Cummings, J. L. Alzheimer's Disease. *N. Engl. J. Med.* **2004**, *351* (1), 56–67. https://doi.org/10.1056/NEJMra040223.

(94)   Fändrich, M.; Meinhardt, J.; Grigorieff, N. Structural Polymorphism of Alzheimer Abeta and Other Amyloid Fibrils. *Prion*. 2009, pp 89–93.

https://doi.org/10.4161/pri.3.2.8859.

(95)   Xi, W.; Wang, W.; Abbott, G.; Hansmann, U. H. E. Stability of a Recently Found Triple-β-Stranded Aβ1-42 Fibril Motif. *J. Phys. Chem. B* **2016**, *120* (20), 4548–4557. https://doi.org/10.1021/acs.jpcb.6b01724.

(96)   Liu, Y.; Ren, B.; Zhang, Y.; Sun, Y.; Chang, Y.; Liang, G.; Xu, L.; Zheng, J. Molecular Simulation Aspects of Amyloid Peptides at Membrane Interface. *Biochimica et Biophysica Acta - Biomembranes*. Elsevier September 1, 2018, pp 1906–1916. https://doi.org/10.1016/j.bbamem.2018.02.004.

(97)   Brown, A. M.; Bevan, D. R. Influence of Sequence and Lipid Type on Membrane Perturbation by Human and Rat Amyloid β-Peptide (1–42). *Arch. Biochem. Biophys.* **2017**, *614*, 1–13. https://doi.org/10.1016/j.abb.2016.11.006.

(98)   Liu, Y.; Ren, B.; Zhang, Y.; Sun, Y.; Chang, Y.; Liang, G.; Xu, L.; Zheng, J. Molecular Simulation Aspects of Amyloid Peptides at Membrane Interface. *Biochimica et Biophysica Acta - Biomembranes*. Elsevier September 1, 2018, pp 1906–1916. https://doi.org/10.1016/j.bbamem.2018.02.004.

(99)   Parton, D. L.; Klingelhoefer, J. W.; Sansom, M. S. P. Aggregation of Model Membrane Proteins, Modulated by Hydrophobic Mismatch, Membrane Curvature, and Protein Class. *Biophys. J.* **2011**, *101* (3), 691–699. https://doi.org/10.1016/j.bpj.2011.06.048.

(100) Mason, R. P.; Jacob, R. F.; Walter, M. F.; Mason, P. E.; Avdulov, N. A.; Chochina, S. V; Igbavboa, U.; Wood, W. G. Distribution and Fluidizing Action of Soluble and Aggregated Amyloid β- Peptide in Rat Synaptic Plasma Membranes. *J. Biol. Chem.* **1999**, *274* (26), 18801–18807. https://doi.org/10.1074/jbc.274.26.18801.

(101) Guerrini, R.; Tomaselli, S.; Crescenzi, O.; Picone, D.; Temussi, P. A.; D'Ursi, A. M.; Salvadori, S. Solution Structure of the Alzheimer Amyloid β-Peptide (1-42) in an Apolar Microenvironment. *Eur. J. Biochem.* **2003**, *269* (22), 5642–5648. https://doi.org/10.1046/j.1432-1033.2002.03271.x.

(102) Xiao, Y.; Ma, B.; McElheny, D.; Parthasarathy, S.; Long, F.; Hoshi, M.; Nussinov, R.; Ishii, Y. Aβ(1-42) Fibril Structure Illuminates Self-Recognition and Replication of Amyloid in Alzheimer's Disease. *Nat. Struct. Mol. Biol.* **2015**, *22* (6), 499–505. https://doi.org/10.1038/nsmb.2991.

(103) Brown, A. M.; Bevan, D. R. Molecular Dynamics Simulations of Amyloid β-Peptide (1-42): Tetramer Formation and Membrane Interactions. *Biophys. J.* **2016**, *111* (5), 937–949. https://doi.org/10.1016/j.bpj.2016.08.001.

(104) Lee, J.; Cheng, X.; Swails, J. M.; Yeom, M. S.; Eastman, P. K.; Lemkul, J. A.; Wei, S.; Buckner, J.; Jeong, J. C.; Qi, Y.; et al. CHARMM-GUI Input Generator for NAMD, GROMACS, AMBER, OpenMM, and CHARMM/OpenMM Simulations Using the CHARMM36 Additive Force Field. *J. Chem. Theory Comput.* **2016**, *12* (1), 405–413. https://doi.org/10.1021/acs.jctc.5b00935.

(105) Brooks, B. R.; Brooks, C. L.; Mackerell, A. D.; Nilsson, L.; Petrella, R. J.; Roux, B.; Won, Y.; Archontis, G.; Bartels, C.; Boresch, S.; et al. CHARMM: The Biomolecular Simulation Program. *J. Comput. Chem.* **2009**, *30* (10), 1545–1614. https://doi.org/10.1002/jcc.21287.

(106) Jo, S.; Kim, T.; Iyer, V. G.; Im, W. CHARMM-GUI: A Web-Based Graphical User Interface for CHARMM. *J. Comput. Chem.* **2008**, *29* (11), 1859–1865. https://doi.org/10.1002/jcc.20945.

(107) Abraham, M. J.; Murtola, T.; Schulz, R.; Páll, S.; Smith, J. C.; Hess, B.; Lindah, E. Gromacs: High Performance Molecular Simulations through Multi-Level Parallelism from Laptops to Supercomputers. *SoftwareX* **2015**, *1–2*, 19–25. https://doi.org/10.1016/j.softx.2015.06.001.

(108) Huang, J.; Rauscher, S.; Nawrocki, G.; Ran, T.; Feig, M.; De Groot, B. L.; Grubmüller, H.; MacKerell, A. D. CHARMM36m: An Improved Force Field for Folded and Intrinsically Disordered Proteins. *Nat. Methods* **2016**, *14* (1), 71–73. https://doi.org/10.1038/nmeth.4067.

(109) Jorgensen, W. L.; Chandrasekhar, J.; Madura, J. D.; Impey, R. W.; Klein, M. L. Comparison of Simple Potential Functions for Simulating Liquid Water. *J. Chem. Phys.* **1983**, *79* (2), 926–935. https://doi.org/10.1063/1.445869.

(110) Wang, J.; Li, J.; Deng, N.; Zhao, X.; Liu, Y.; Wang, X.; Zhang, H. Transfection of HBMP-2 into Mesenchymal Stem Cells Derived from Human Umbilical Cord Blood and Bone Marrow Induces Cell Differentiation into Chondrocytes. *Minerva Med.* **2014**, *105* (4), 283–288. https://doi.org/10.1063/1.464397.

(111) Bussi, G.; Donadio, D.; Parrinello, M. Canonical Sampling through Velocity Rescaling. *J. Chem. Phys.* **2007**, *126* (1), 014101. https://doi.org/10.1063/1.2408420.

(112) Berendsen, H. J. C.; Postma, J. P. M.; Van Gunsteren, W. F.; Dinola, A.; Haak, J. R. Molecular Dynamics with Coupling to an External Bath. *J. Chem. Phys.* **1984**, *81* (8), 3684–3690. https://doi.org/10.1063/1.448118.

(113) Evans, D. J.; Holian, B. L. The Nose-Hoover Thermostat. *J. Chem. Phys.* **1985**, *83* (8), 4069–4074. https://doi.org/10.1063/1.449071.

(114) Allen, W. J.; Lemkul, J. A.; Bevan, D. R. GridMAT-MD: A Grid-Based Membrane Analysis Tool for Use with Molecular Dynamics. *J. Comput. Chem.* **2009**, *30* (12), 1952–1958. https://doi.org/10.1002/jcc.21172.

(115) Janosi, L.; Gorfe, A. A. Simulating POPC and POPC/POPG Bilayers: Conserved Packing and Altered Surface Reactivity. *J. Chem. Theory Comput.* **2010**, *6* (10), 3267–3273. https://doi.org/10.1021/ct100381g.

(116) Plesnar, E.; Subczynski, W. K.; Pasenkiewicz-Gierula, M. Saturation with Cholesterol Increases Vertical Order and Smoothes the Surface of the Phosphatidylcholine Bilayer: A Molecular Simulation Study. *Biochim. Biophys. Acta - Biomembr.* **2012**, *1818* (3), 520–529. https://doi.org/10.1016/j.bbamem.2011.10.023.

(117) Venable, R. M.; Brown, F. L. H.; Pastor, R. W. Mechanical Properties of Lipid Bilayers from Molecular Dynamics Simulation. *Chem. Phys. Lipids* **2015**, *192*, 60–74. https://doi.org/10.1016/j.chemphyslip.2015.07.014.

(118) Iwatsubo, T.; Odaka, A.; Suzuki, N.; Mizusawa, H.; Nukina, N.; Ihara, Y. Visualization of Aβ42(43) and Aβ40 in Senile Plaques with End-Specific Aβ Monoclonals: Evidence That an Initially Deposited Species Is Aβ42(43). *Neuron* **1994**, *13* (1), 45–53. https://doi.org/10.1016/0896-6273(94)90458-8.

(119) Zhao, L. N.; Long, H.; Mu, Y.; Chew, L. Y. The Toxicity of Amyloid β Oligomers. *International Journal of Molecular Sciences*. Multidisciplinary Digital Publishing Institute (MDPI) 2012, pp 7303–7327. https://doi.org/10.3390/ijms13067303.

(120) Kučerka, N.; Tristram-Nagle, S.; Nagle, J. F. Structure of Fully Hydrated Fluid Phase Lipid Bilayers with Monounsaturated Chains. *J. Membr. Biol.* **2006**, *208* (3), 193–202. https://doi.org/10.1007/s00232-005-7006-8.

(121) Elmore, D. E. Molecular Dynamics Simulation of a Phosphatidylglycerol Membrane. *FEBS Lett.* **2006**, *580* (1), 144–148. https://doi.org/10.1016/j.febslet.2005.11.064.

(122) Kučerka, N.; Tristram-Nagle, S.; Nagle, J. F. Structure of Fully Hydrated Fluid Phase Lipid Bilayers with Monounsaturated Chains. *J. Membr. Biol.* **2006**, *208* (3), 193–202. https://doi.org/10.1007/s00232-005-7006-8.

(123) Nagle, J. F. Experimentally Determined Tilt and Bending Moduli of Single-Component Lipid Bilayers. *Chemistry and Physics of Lipids*. June 2017, pp 18–24. https://doi.org/10.1016/j.chemphyslip.2017.04.006.

Supporting information to chapter 4

S 4.1. System configuration

While the peptide and the oligomer are oriented randomly inside the membrane, the fibre is oriented in four various ways to obtain different replicas. In particular, the principal axis of the protein is aligned along x axis, which is denoted as horizontal, along z axis, denoted as vertical and along two diagonal, differentiated into diagonal + and diagonal – (Figure S 1).
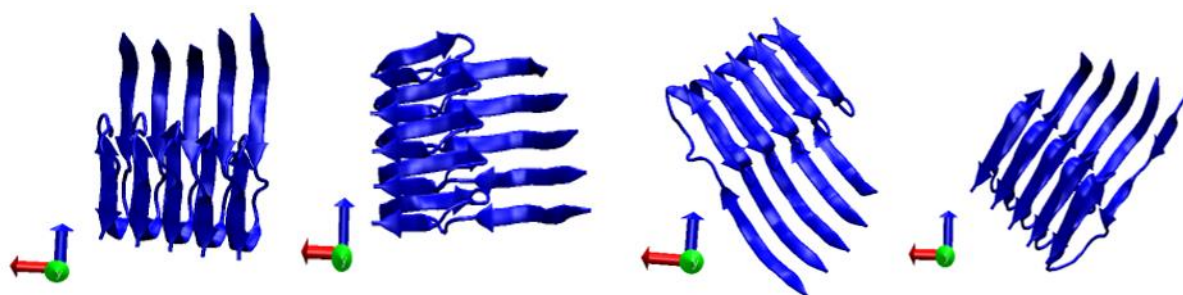
Figure S 1 – To obtain different replicas, the fibre is oriented in four directions, from the left: along x-axis, along z-axis, and on two diagonal, denoted respectively diagonal- and diagonal+.

In Table S 1 each system with the number of interacting particles is summarized.

Table S 1

SYSTEM	PROTEIN	POPC	TIP3	IONS	ATOMS
ONLY MEMBRANE	0	574	6264	26	95734
PEPTIDE	1	567	7905	39	100210
OLIGOMER	5	552	21804	115	141885
HORIZONTAL	5	554	33434	183	177111
VERTICAL	5	542	25354	139	151219
DIAGONAL +	5	553	32432	181	173969
DIAGONAL -	5	553	31875	177	172294

S 4.2. Vectors definition for Order Parameter and Splay angle calculation

Figure S 2 shows how to obtain the vector $\vec{a}$, used in the calculation of the order parameter and the splay angle. $\vec{a}$ connects the center of mass of headgroups (P-C2) and the center of mass of the three terminal carbons on the two lipid tails (C216 – C217 – C218 – C314 – C315 – C316).
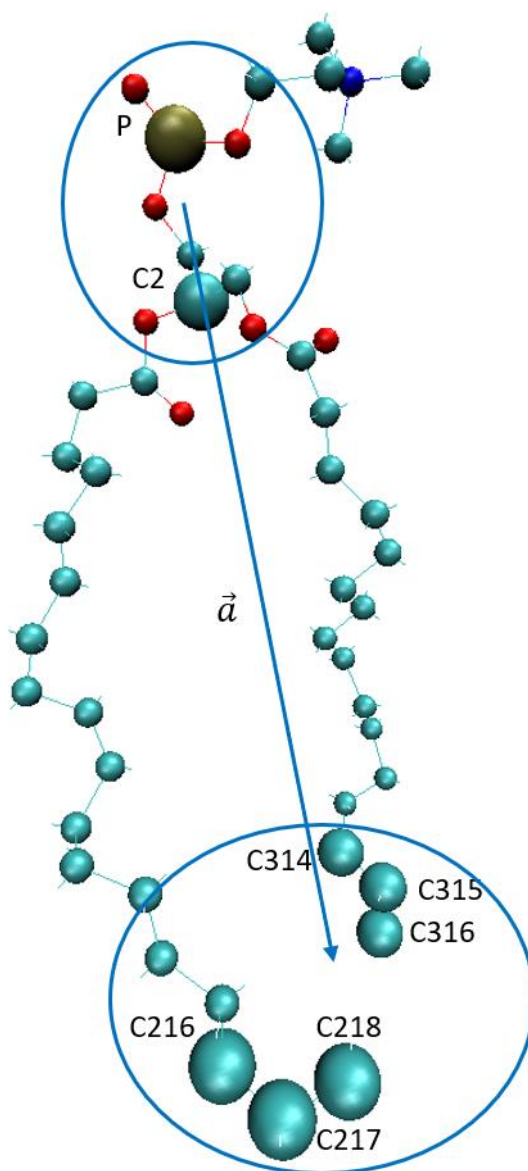

Figure S 2 – Graphical representation of the vector $\vec{a}$ used to calculate bending modulus and order parameter

In Figure S 3 the normalized probability distributions and the PMF profiles used in the bending modulus calculation are shown.
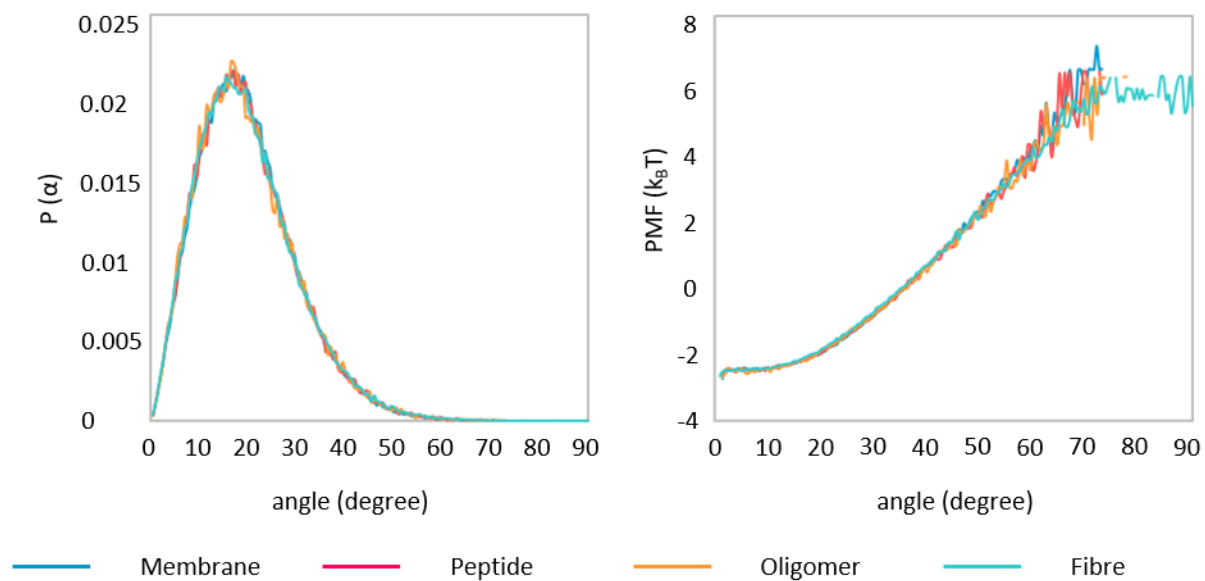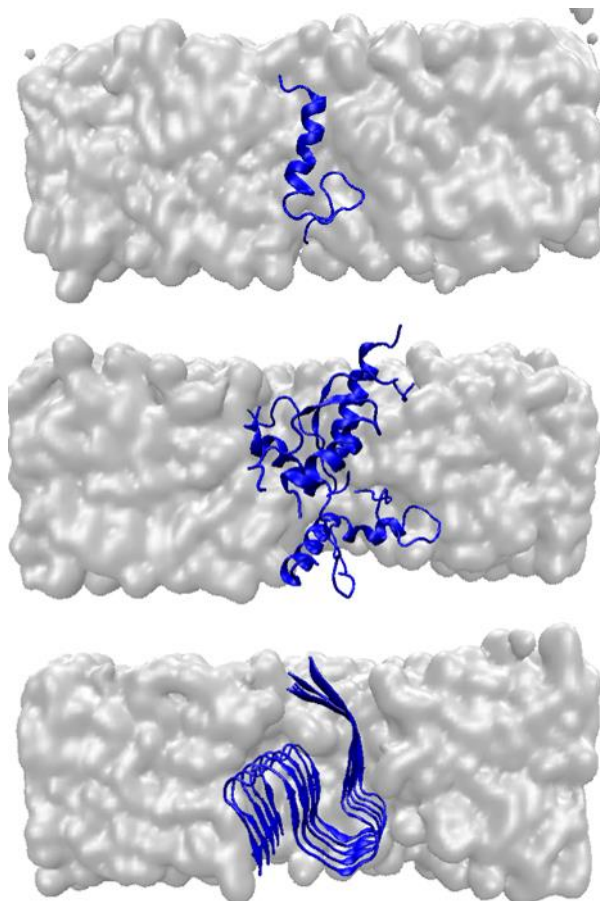

Figure S 3 – Graphs display the normalized probability distribution of splay angle and the PMF used to calculate the bending modulus.

S 4.3. Results

In Figure S 4 are reported initial configurations of the systems where the protein is embedded into the bilayer.

Figure S 4 – Representation of the initial states for each system analysed. From the top there is the peptide, the oligomer and the fibre.